3D diamond timing detectors- attività WP2

Timespot meeting- Cagliari-1 Dicembre 2017

Silvio Sciortino
Dipartimento di Fisica e INFN di Firenze

1. Caratterizzazione preliminare di campioni monocristallini (E6, IIa) ,
policristallini (E6, II-VI),
eteroepitassiali (Audiatec).
Misura di Charge Collection Effiecncy con sorgente beta
(^{90} Sr)

2. Update del sistema laser di fabbricazione degli elettrodi colonnari: ottimizzazione dell'aspect ratio, della resistività elettrica

3. Misure di spettrocopia Raman e di resistività sul materiale modificato (grafitico), a seguito dell'upgrade

4. Realizzazione di una procedura di connessione dei sensori con l'elettronica.
Connessione di cammini grafitici superficiali tramite:
(i) wire bonding diretto su grafite;
(ii) metallizazione con scrittura laser di maschere;
(iii) saldatura metallo-diamante?

5. Fabbricazione di sensori con geometrie indicate dalle simulazioni (sezione di Perugia)

6. Misure preliminari di timing

7. Misure di radiation hardness (CCE dopo irraggiamento)

Laser fabrication of an all-carbon 3D sensor

columnar electrodes fabricated with a 800 nm Ti:Sa
40-60 fs mode-locked laser

surface electrodes fabricated with a 1064 nm
Nd:YAG Q-switched 8 ns laser

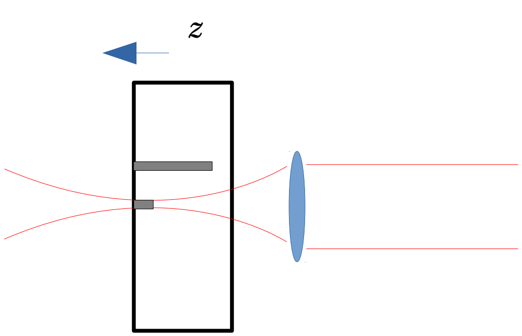

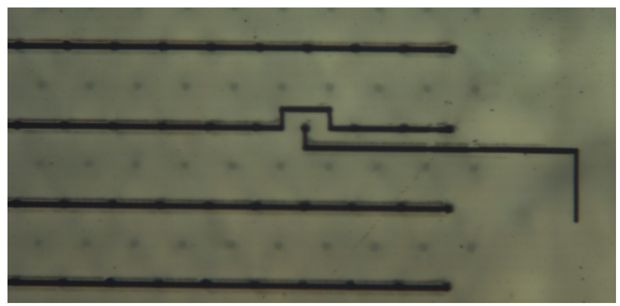

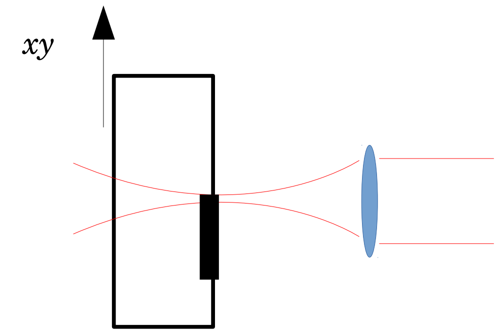

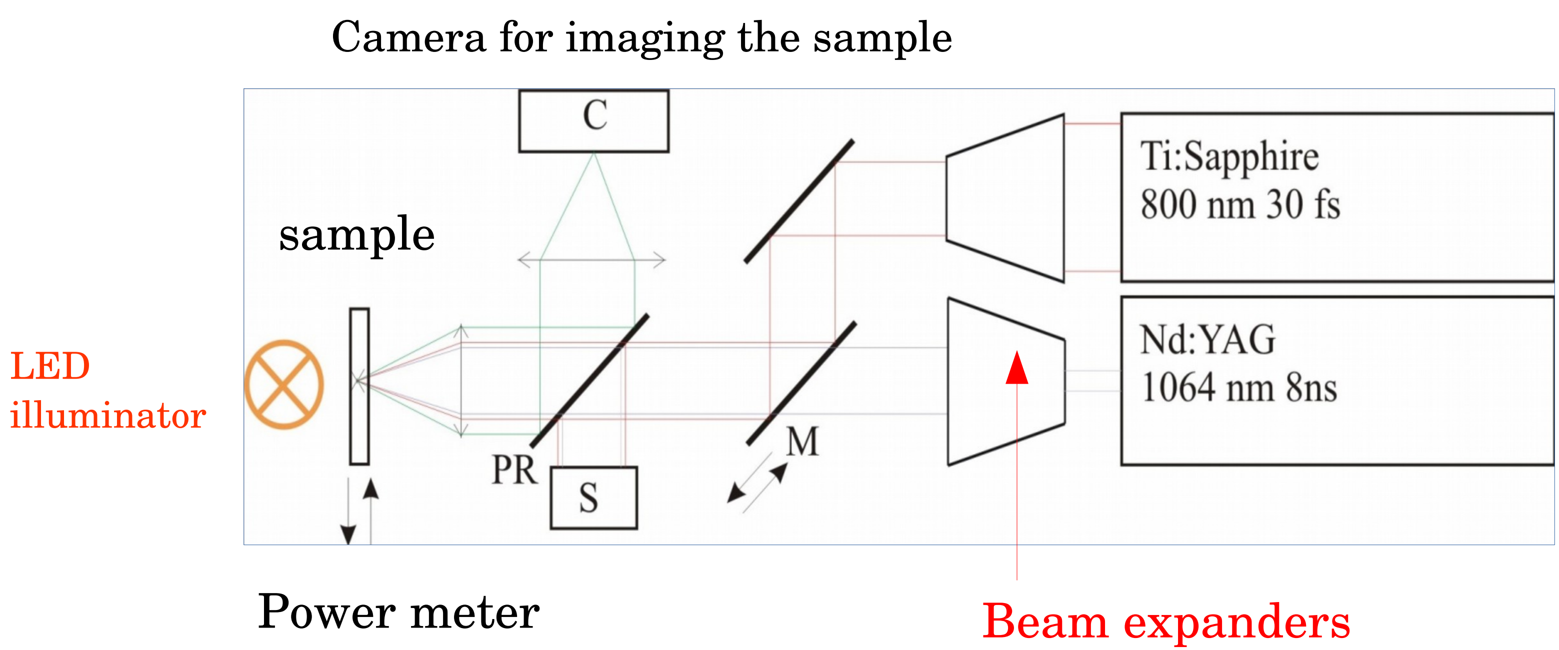

Prepared sensors: 3D sensors monocrystalline plates (Element Six)

4.5x4.5x0.5 mm^3 electronic grade samples

2D reference structure

3D 125 col/mm²

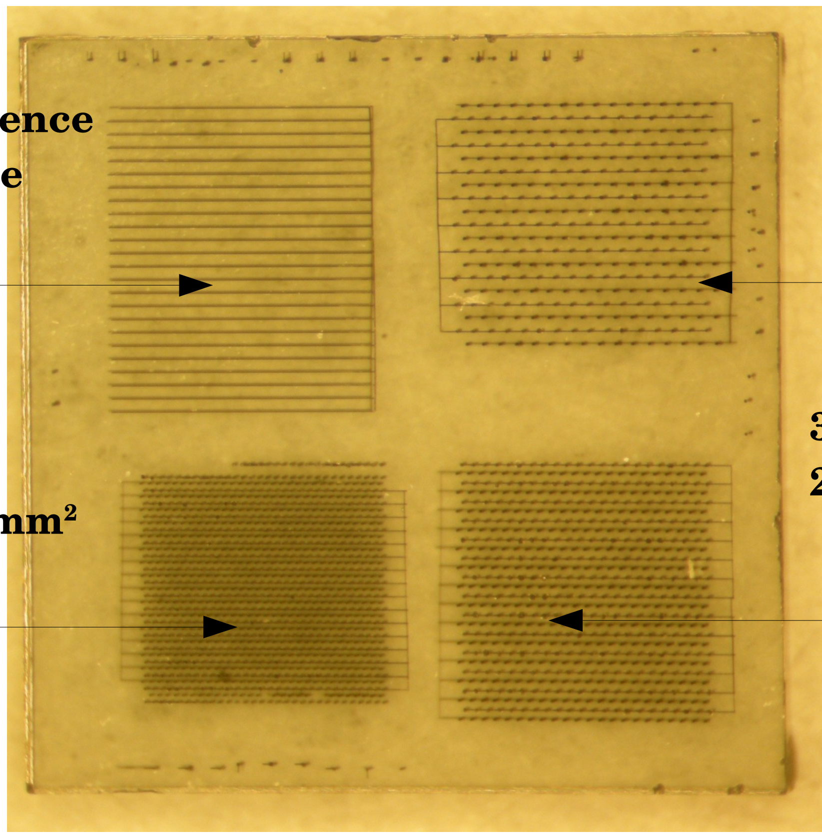

3D 500 col/mm²

3D 250 col/mm²

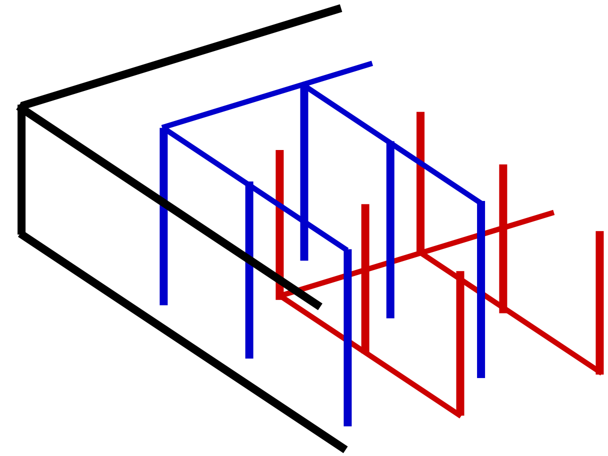

unit cell

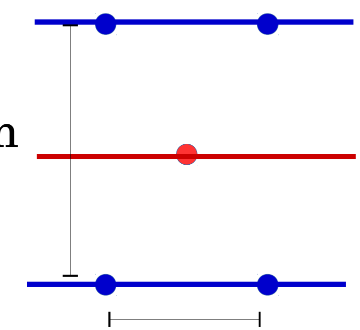

160, 114, 80 um

100, 70, 50 um

a reference sample and three different 3D detectors, connected with surface graphite paths **(columns connected in parallel)**

Charge collection efficiency measurements (CCE) with Minimum Ionizing Particles (MIP): electrons from a β source

Full charge collection

@ 30 V 2D sensor

@ 3 V 3D sensor

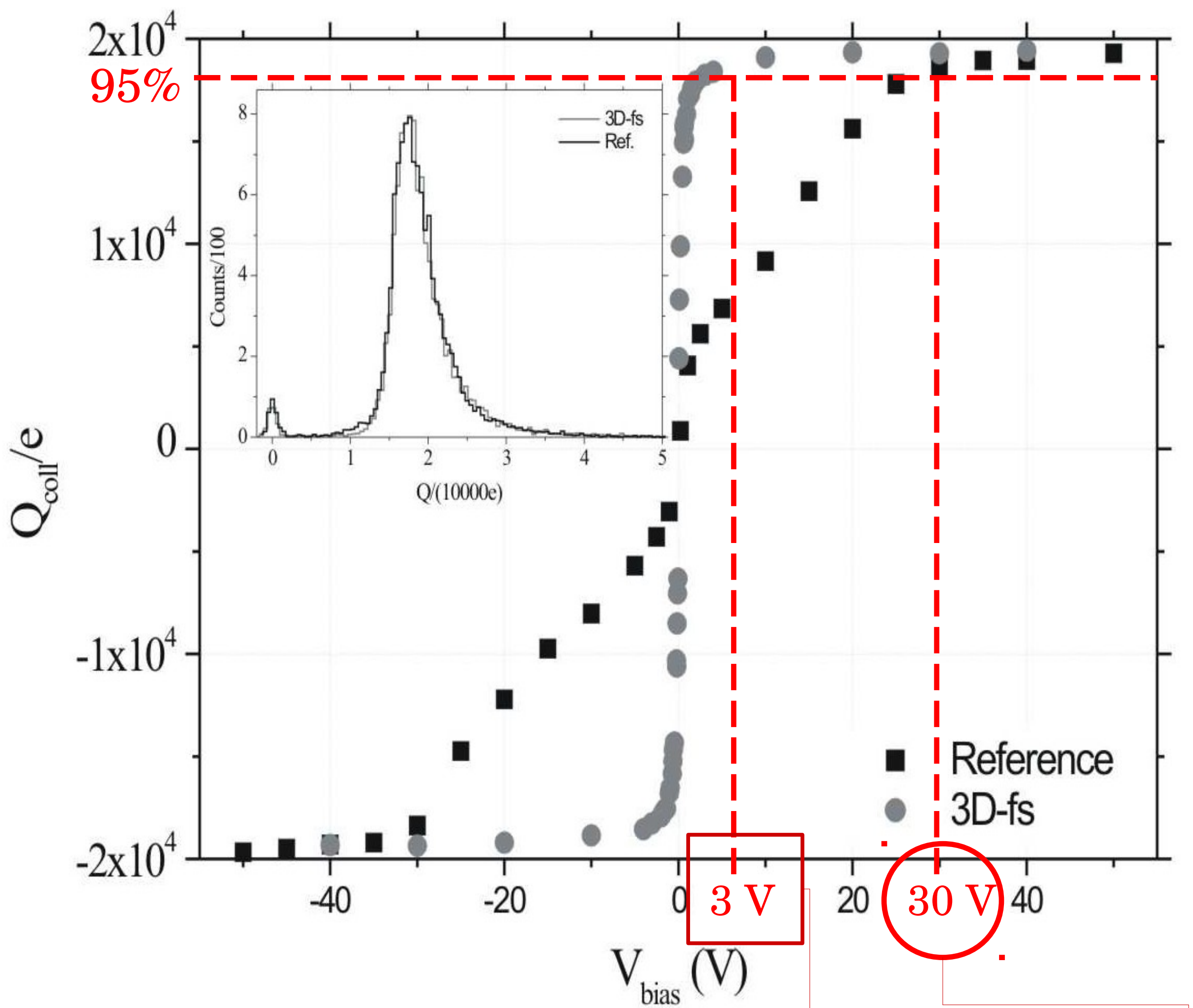

S. Lagomarsino, M. Bellini, C. Corsi, F. Gorelli, G. Parrini, M. Santoro, and S. Sciortino, Three-dimensional diamond detectors: Charge collection efficiency of graphitic electrodes, Appl. Phys. Lett. 103 (2013) 233507 ; doi: 10.1063/1.4839555.

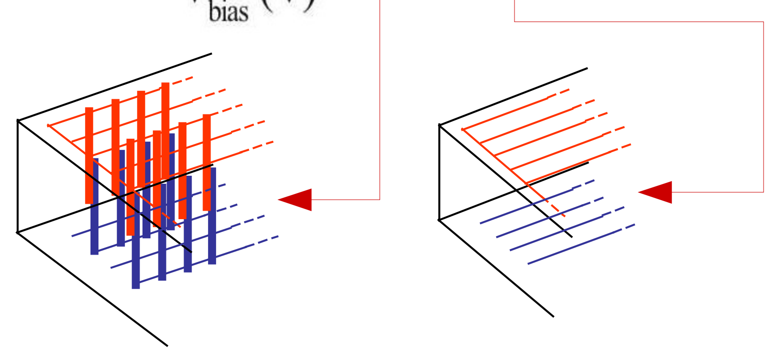

3D sensors on polycrystalline samples

(E6, II-VI)

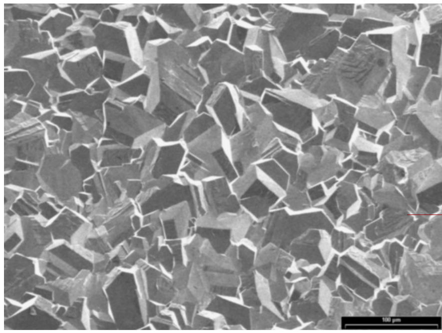

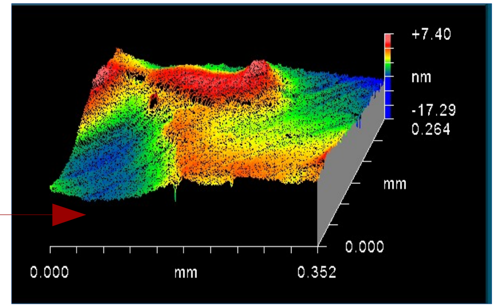

3 structures for each sample

2D

3D 250 col/mm²

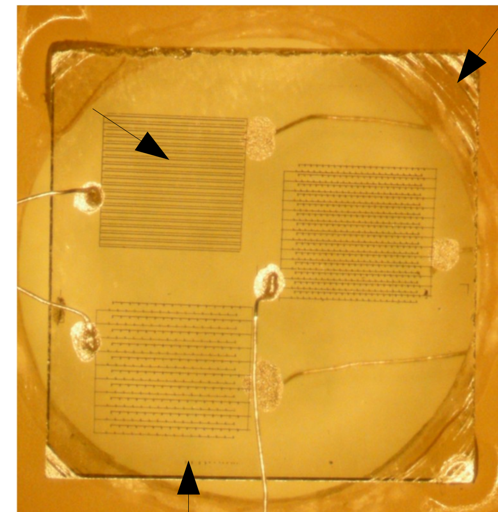

3D 125 col/mm²

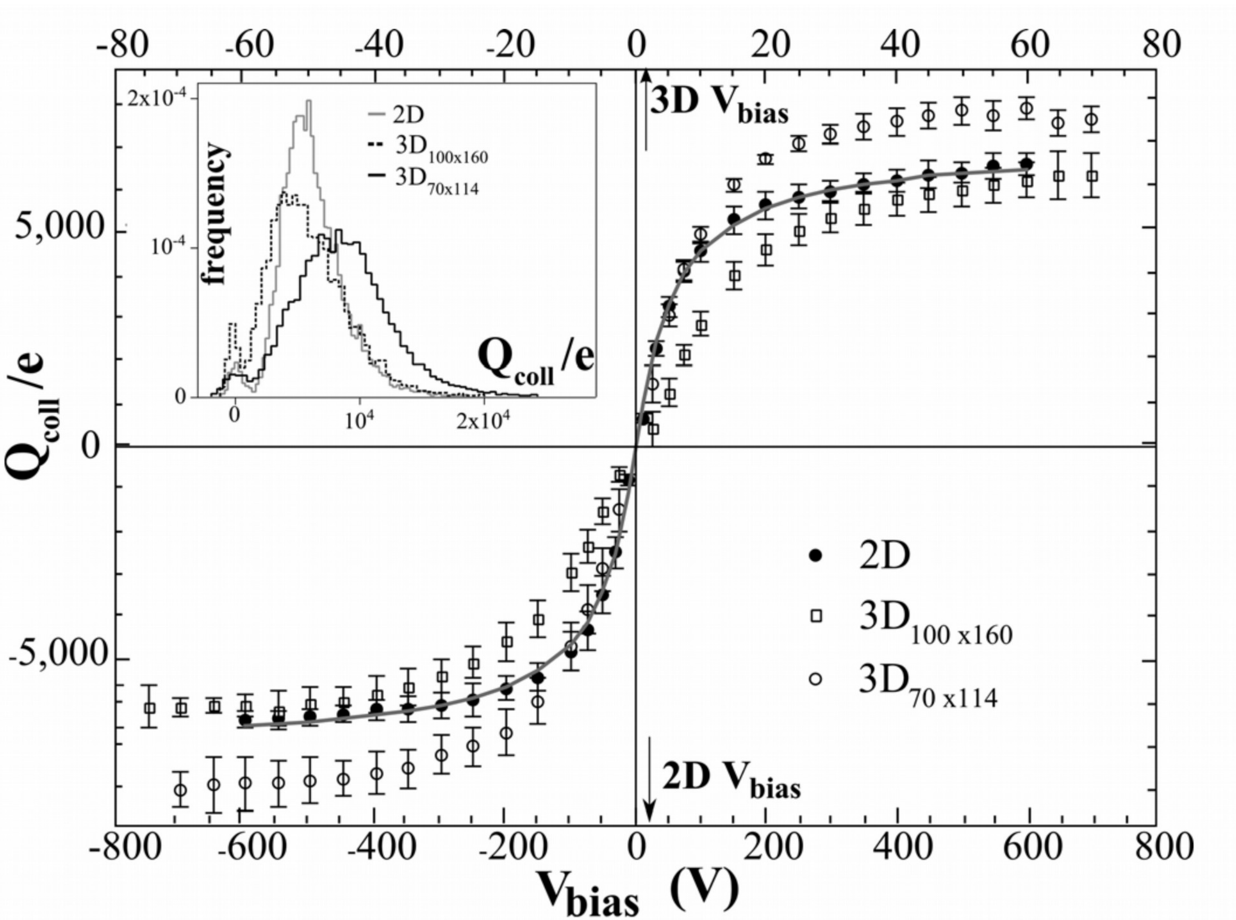

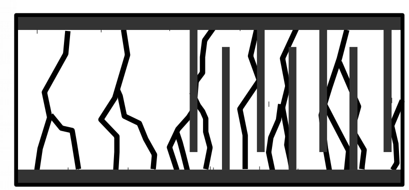

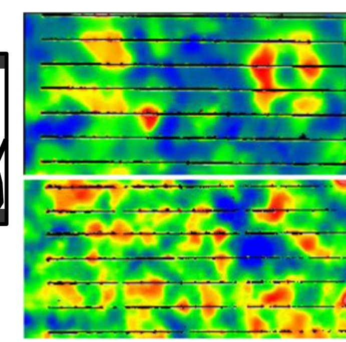

Diamond (heteroepitaxially grown) on Iridium (DOI) at the Univesrity of Augsburg (spin-off Audiatec)

Scientific Reports | 7:44462 |
DOI: 10.1038/srep44462

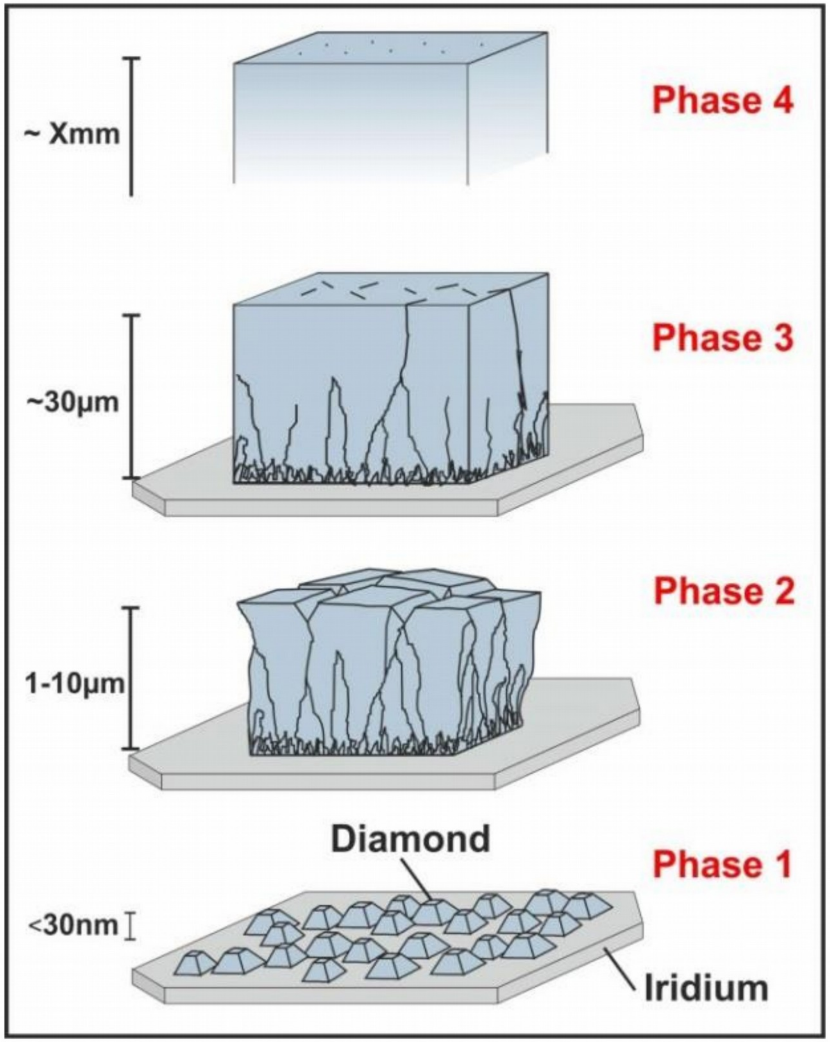

dislocation density inversely proportional to sample thickness

network of grain boundaries dissolves, leaving dislocations

grains merge

nucleation

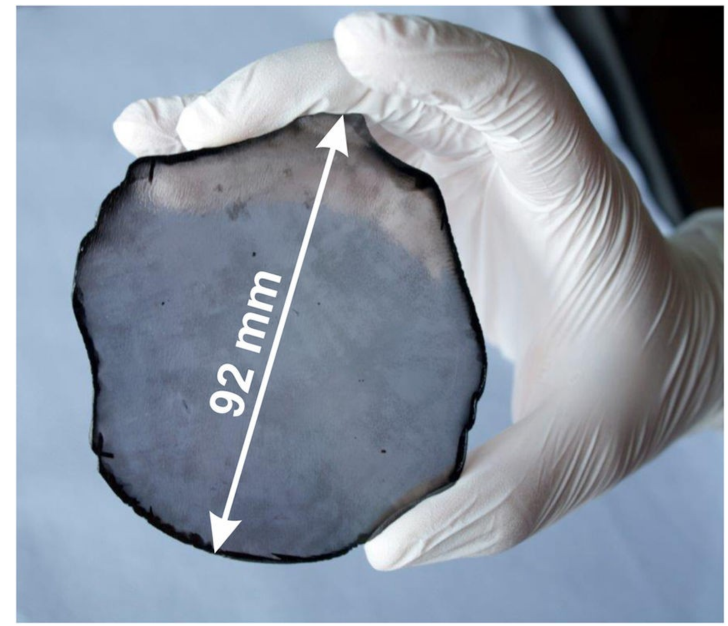

large area, quasi single-crystal

Diamond Detectors Applications for H2020 (network infratructure) spokesperson Mladen Kis, GSI
GSI is a single fund receiver, but can support the activity of material development (possibly free test samples)

Characterization of samples: ^{90}Sr beta source

heteroepitaxial DOI from AUDIATEC and polycrystalline II-VI compared

DOI efficiency equal or higher than the best polyscrystalline samples

The width of the pulse height spectrum distribution is narrower (higher homogeneity)

Pulse Height Spectrum.

DOI sample (n. 2 -3DOSE batch 2017) @ 650 V

thickness (525±10) um, **efficiency @ 1.25 V/um (63±4)%**

Pulse Height Spectrum.

II-VI sample (3DOSE batch 2017) @ 500 V

sample thickness (430±10) um

efficiency @ 1.3 V/um <54 %

a.u.

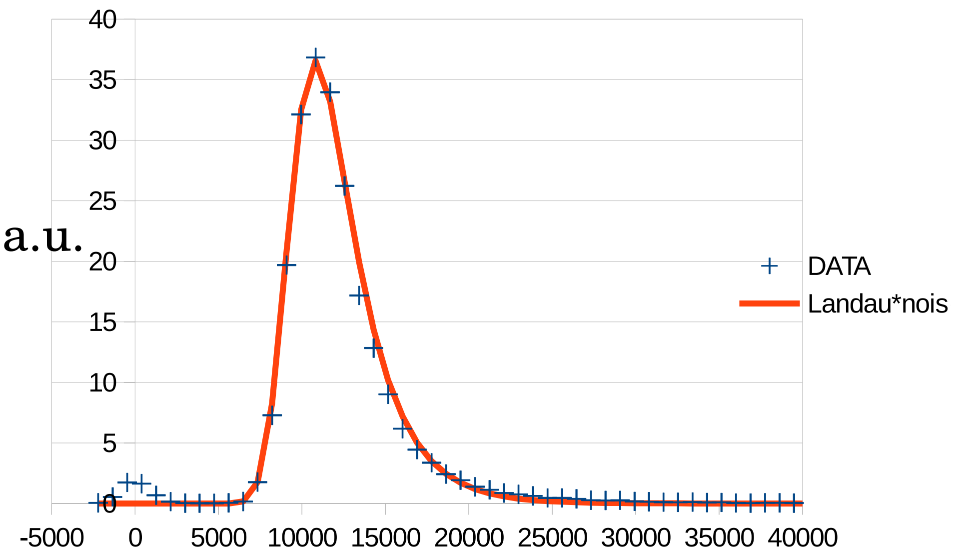

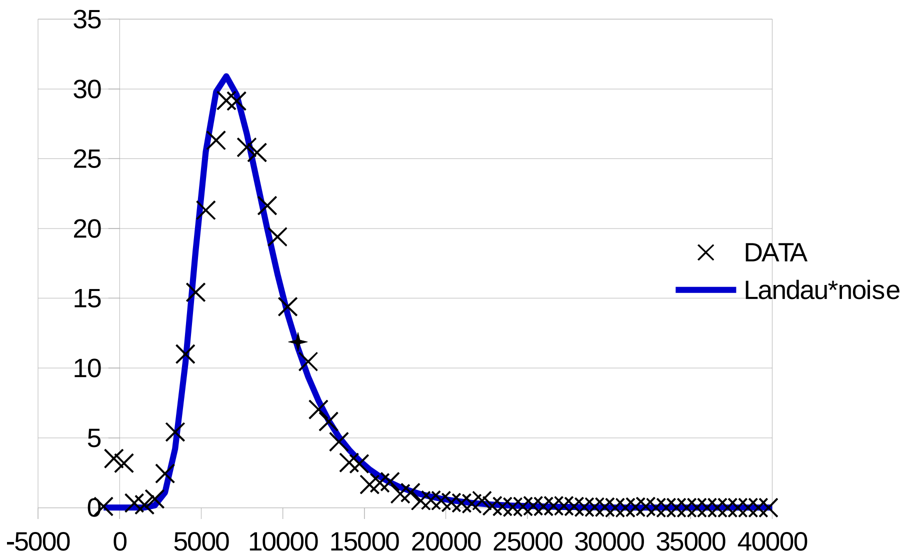

n. of electrons

Preliminary study: DOI sample are polished on the lateral side. This allows to observe the aspect ratio of the columnar electrodes and study them with Raman spectroscopy

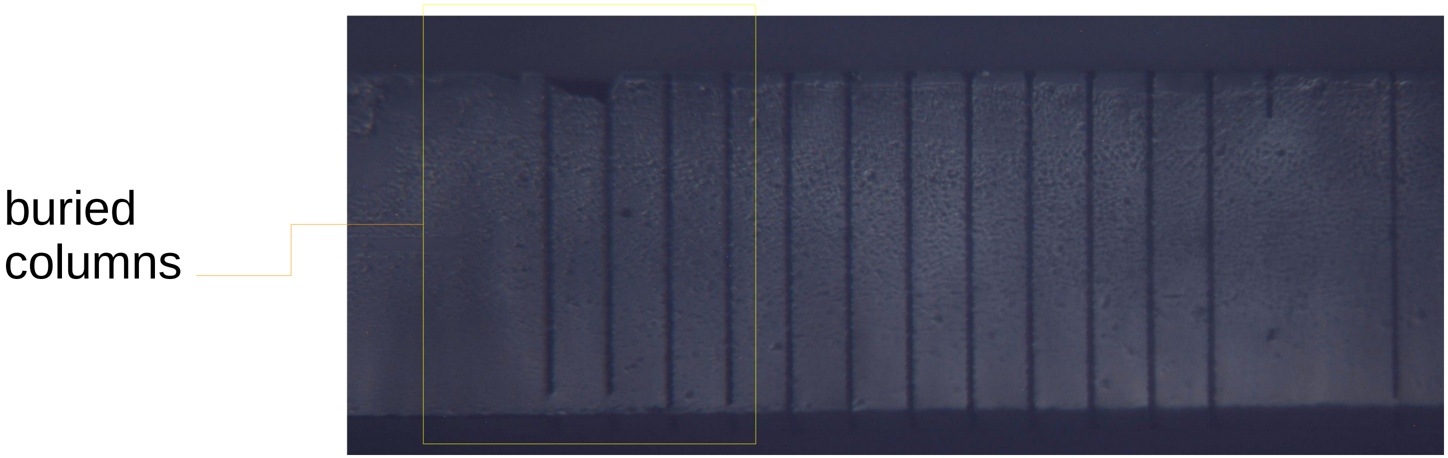

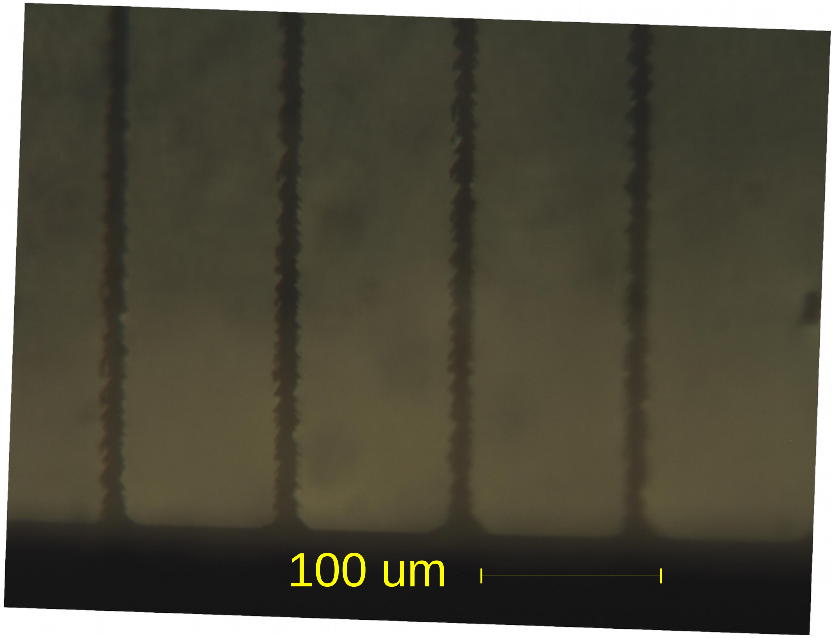

lower resistivity achieved in DOI
is about 1 Ohm cm,
higher than in polycrystalline material

aspect ratio and resistivity to be improved with upgrade of the optical system

Modified material: a mixed sp^2-sp^3 phase

S. Lagomarsino et al., Diamond Relat. Mater., 43:23–28, 2014.

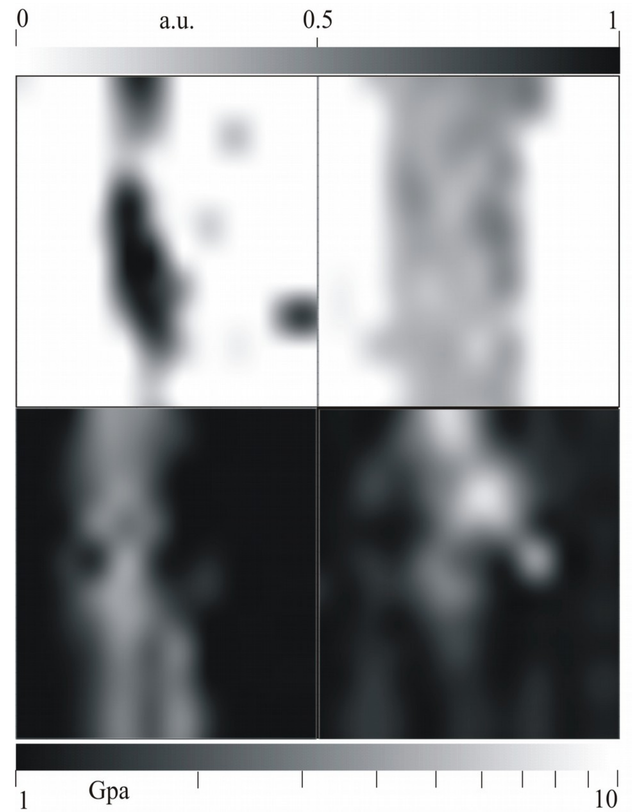

ns laser   fs laser

Ratio between the G peak and the diamond Raman line

Map of the maximum uniaxial pressure corresponding to the same region

Pressure too high for a stable graphitic phase

Resistivity too high, up to 1 Ωcm. *Only surface paths are purely graphitic* sample preparation

(two identical sensors prepared on a DOI and a II-VI poly sample)

Connection with surface conductive paths are in progress

Two arrays of columnar electrodes starting from each side

DOI FRONT SURFACE

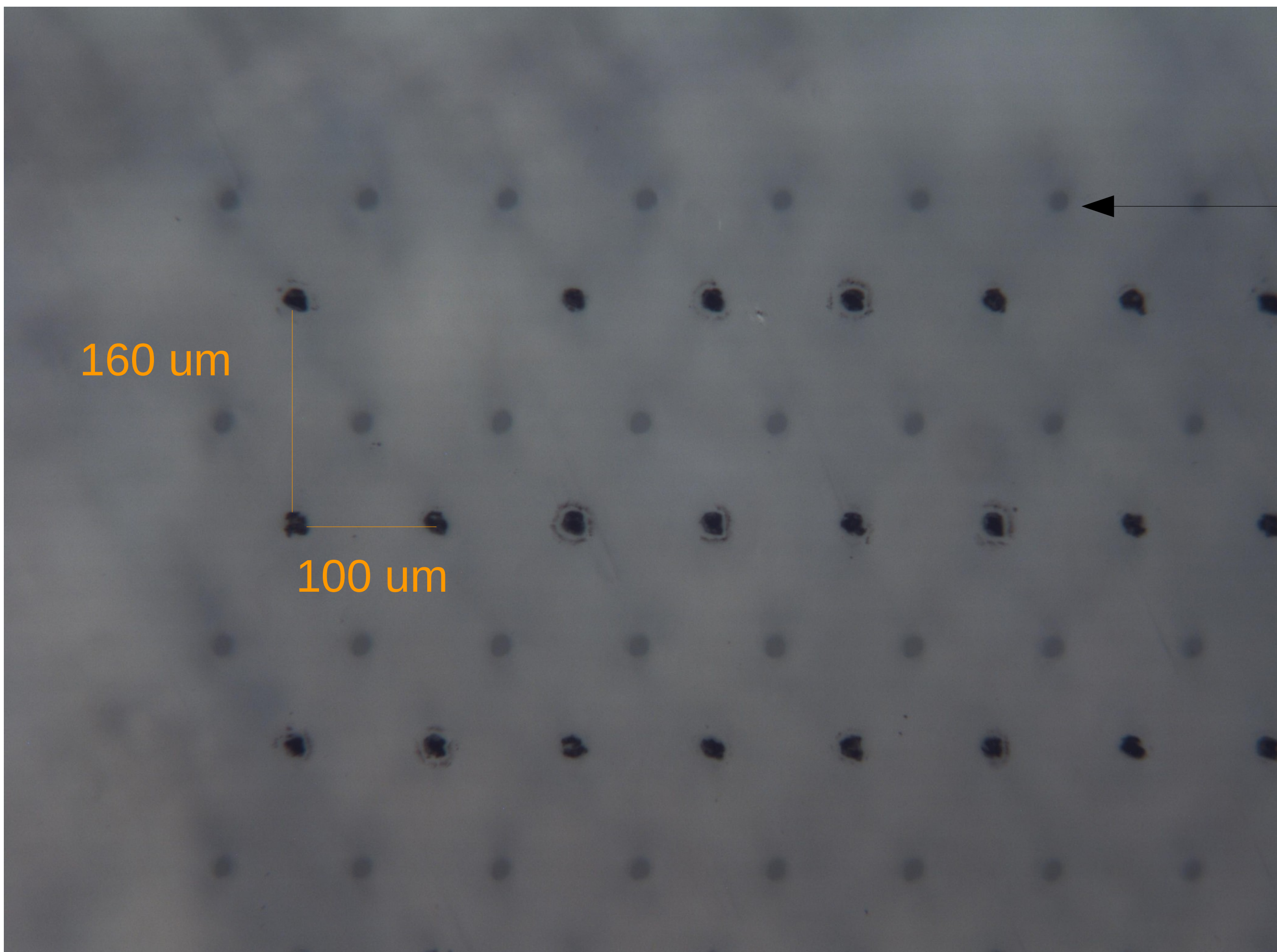

electrode starting form the back side, ending at tens of micrometers form the front surface

electrode starting from the front side

DOI sample tilted

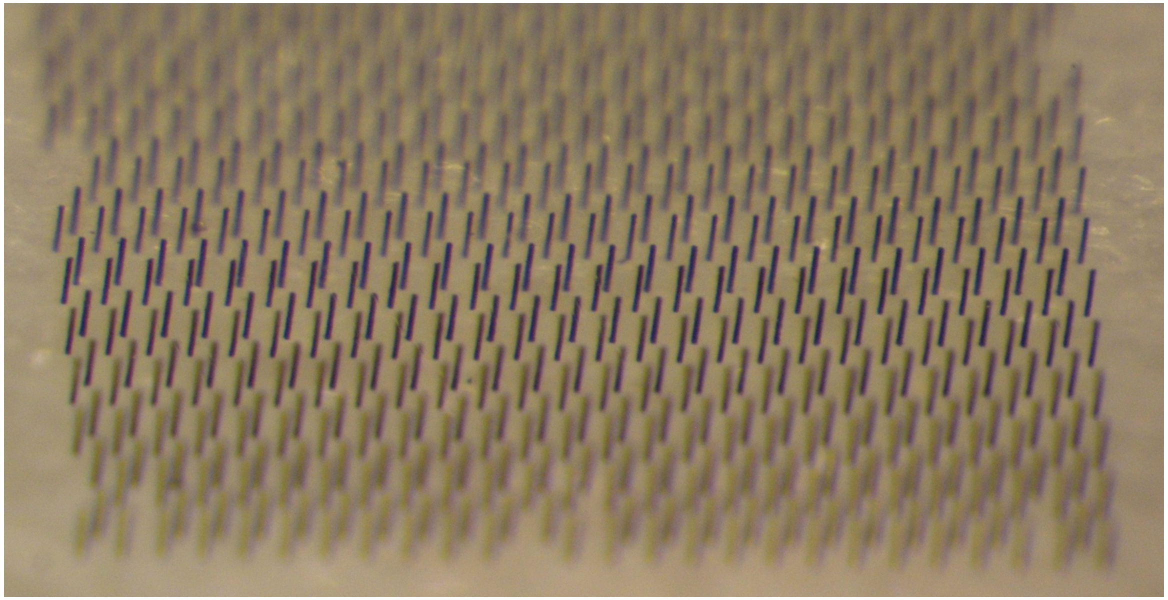

First pixel detector in preparation

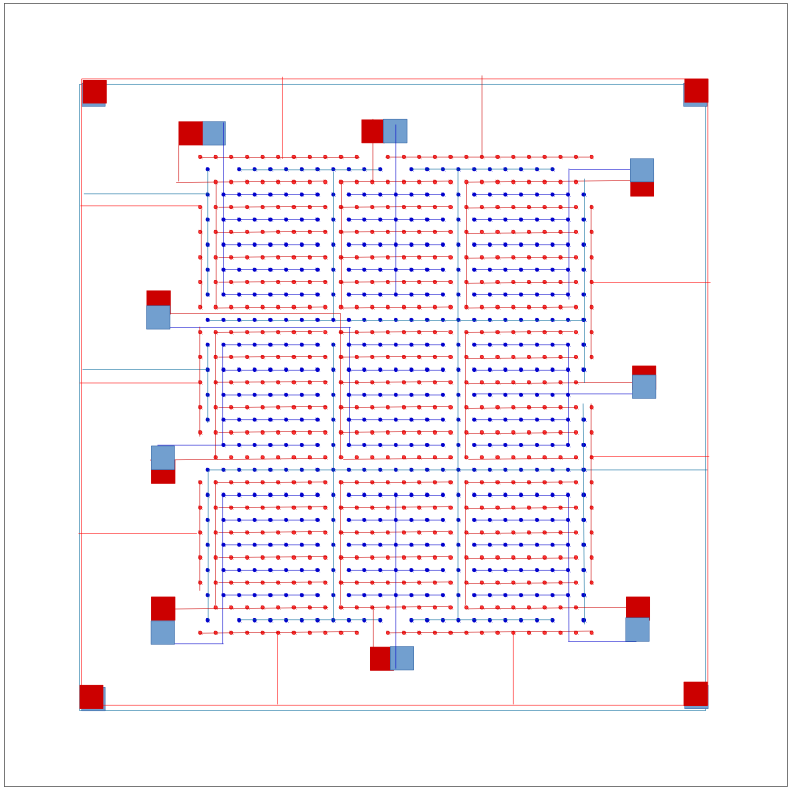

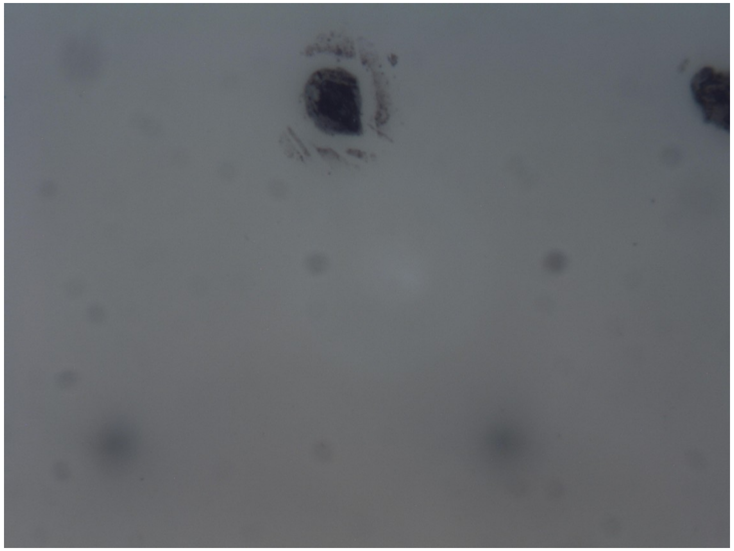

DOI front surface

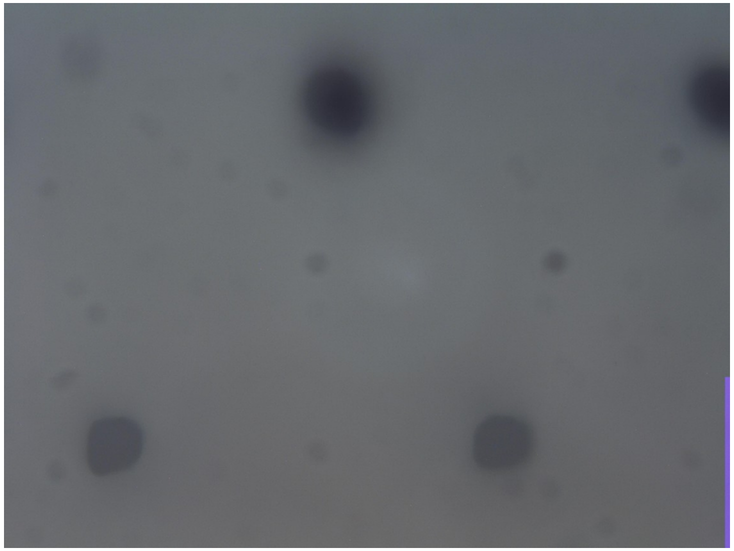

50 um below

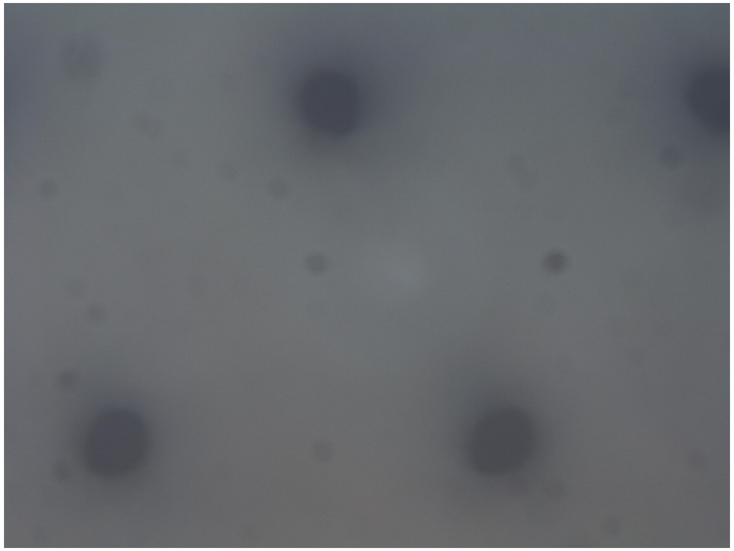

200 um below

electrodes are continuous with a maximum diameter below about 20 um

optimize the parameter to decrease the electrodes diameter

Necessary to correct for spherical aberration

Abnormal resistivity <=1 Ω cm
of the electrodes mainly due to spherical aberration

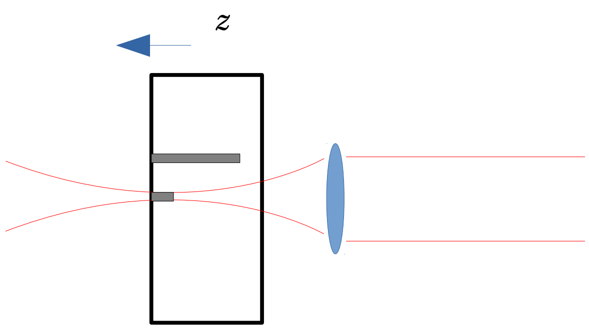

Consequently **the resolution of our first batch was limited to 280 ps**
(CERN-THESIS-2016-016 Development of a timing detector for the TOTEM experiment at the LHC, Minafra, Nicola (INFN, Bari)2016 https://cds.cern.ch/record/2139815?ln=it)

Possibility of lowering the resistivity of about two orders of magnitude (ρ =22 mΩ cm) has been demonstrated **by correcting the wavefront of the laser:**
B. Sun et al. Appl. Phys. Lett. 105, 231105 (2014)

Upgrade

1. Utilizzo di uno specchio deformabile per la correzione delle aberrazioni (già acquistato)
2. Passaggio da un obbiettivo 10 X a un 20 X (maggior definizione del fascio, minor danno locale del reticolo).

DMP40-P01 Integrated Into an Adaptive Optics System

See the table for the list of parts used in the adaptive optics system below. If you hover over a component in the image below, the corresponding item will be highlighted in the table below. This is a sample setup to demonstrate one possilble use of these deformable mirrors, which can also be integrated into other arbitrary setups and controlled with the DMP40 software (download available on the *Software* tab).

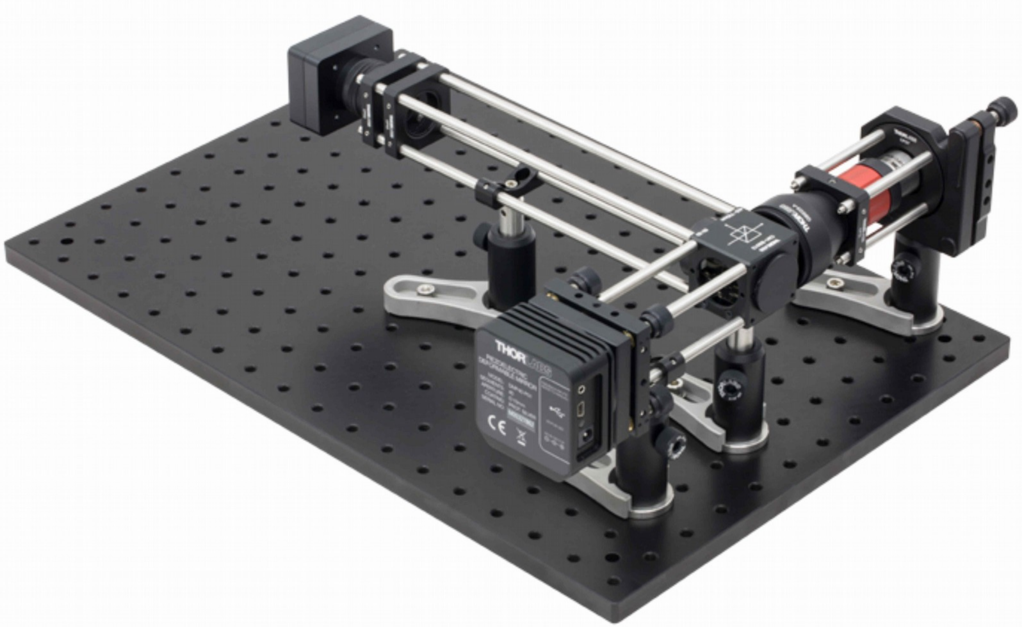

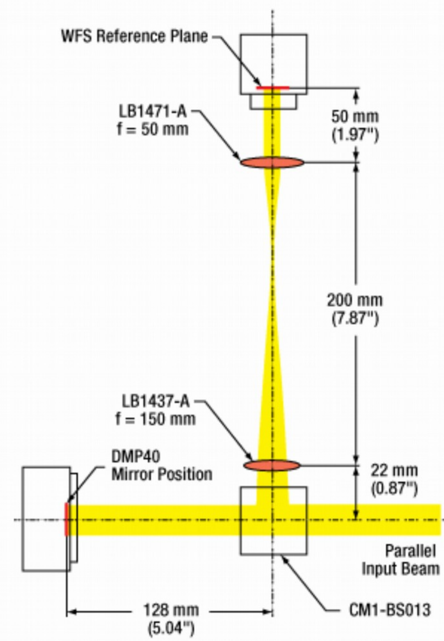

Simplified Diagram of the AO System Shown to the Left

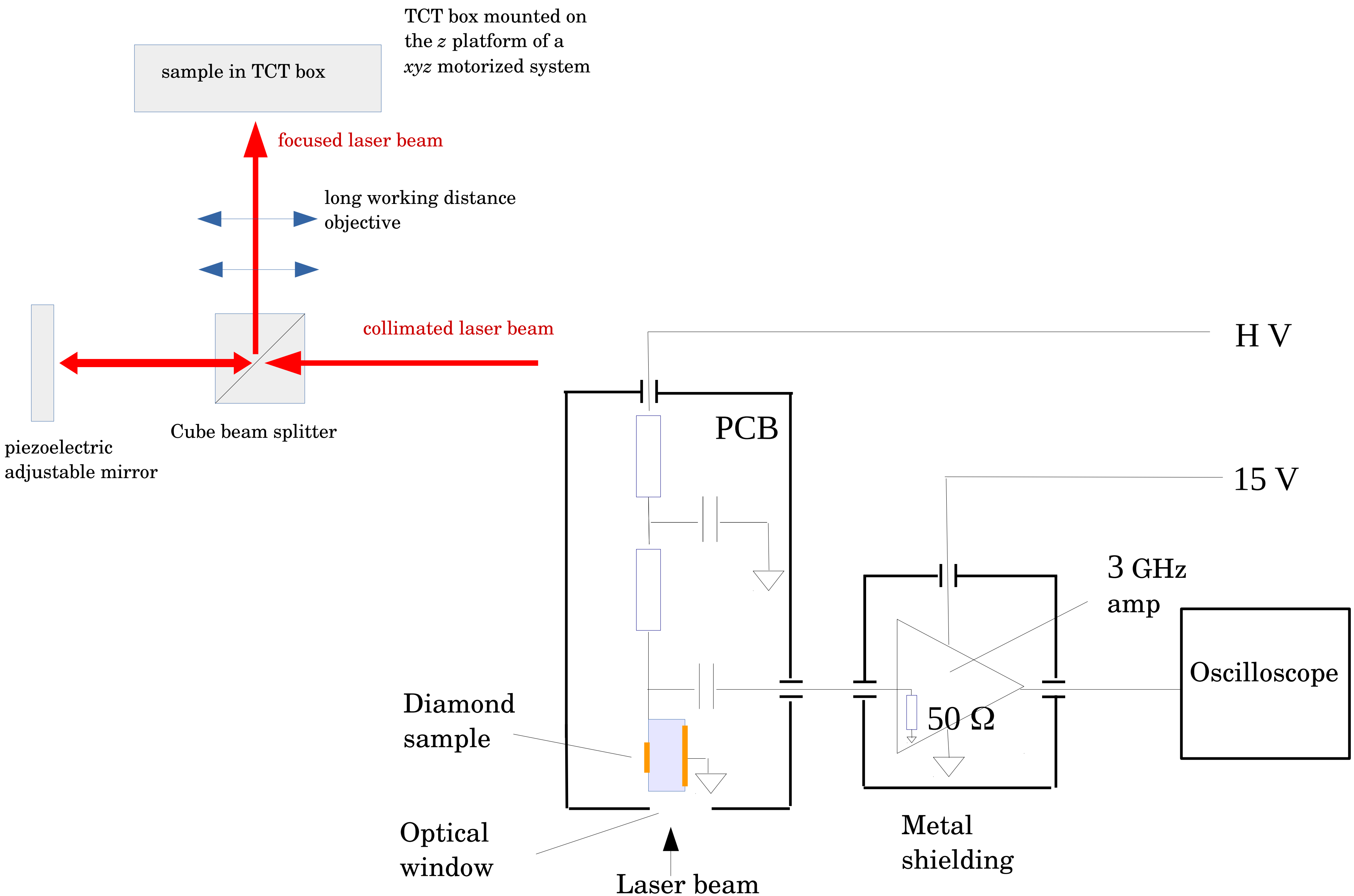

We used an experimental setup used is a slight modification of a reported TCT system: J. Fink, H. Kruger, P. Lodomez, N. Wermes, Nucl. Instr. Meth. A 560 (2006) 435–443.

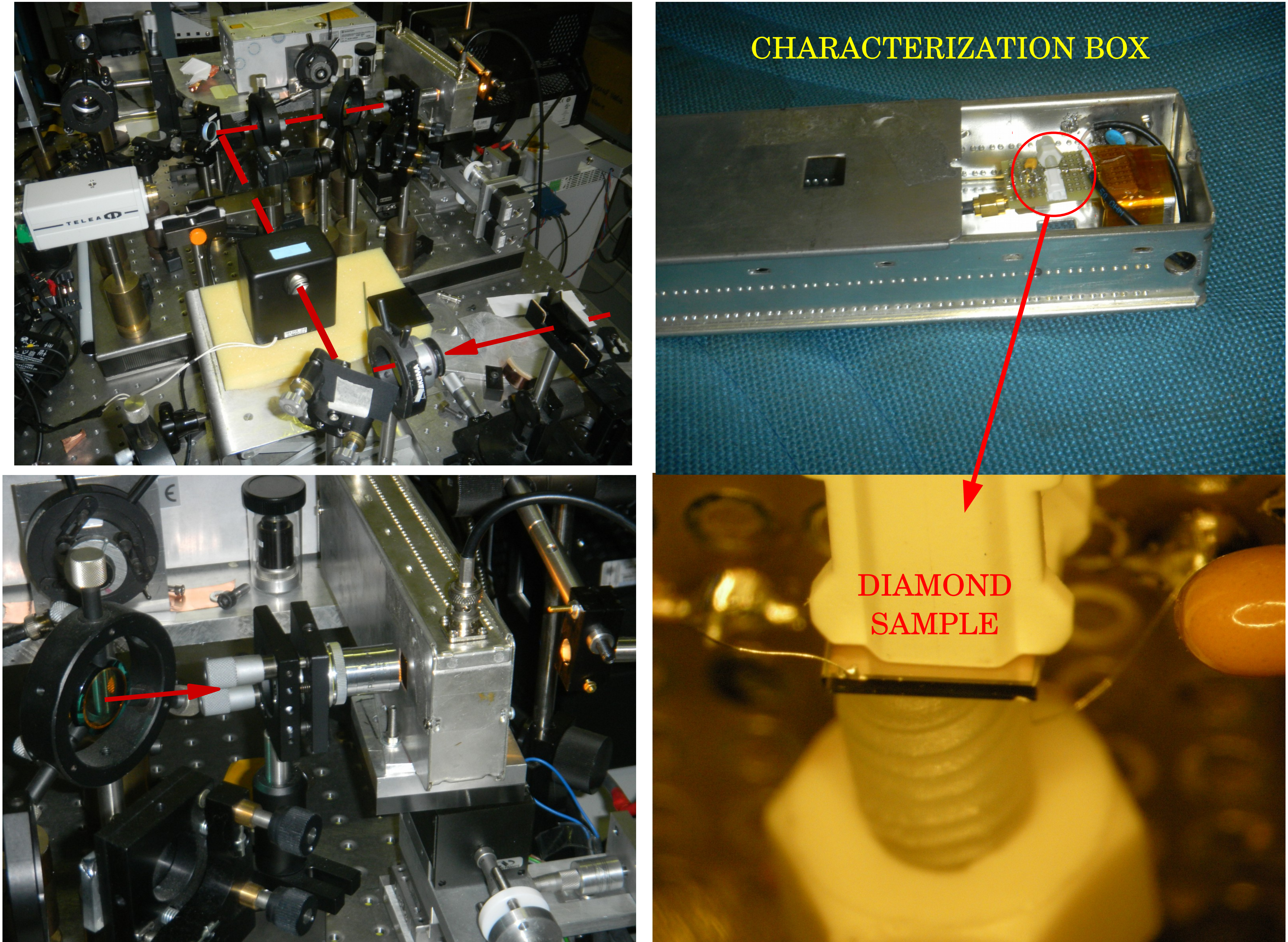
CHARACTERIZATION BOX
DIAMOND SAMPLE

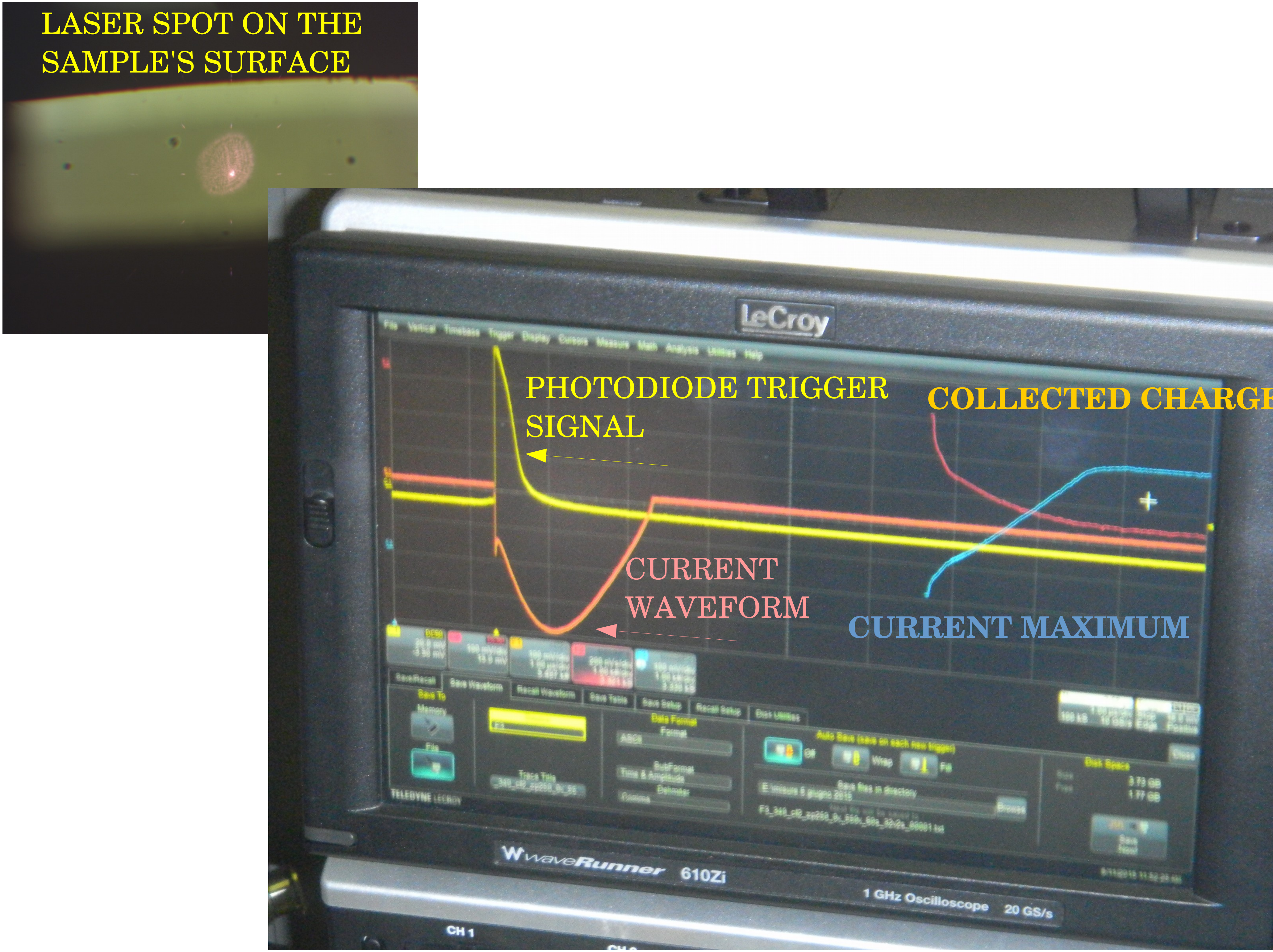
LASER SPOT ON THE SAMPLE'S SURFACE
PHOTODIODE TRIGGER SIGNAL
COLLECTED CHARGE
CURRENT WAVEFORM
CURRENT MAXIMUM
LeCroy
waveRunner 610Zi
1 GHz Oscilloscope 20 GS/s
CH 1

bonding grafite diamnte dimostrato nell'ambito dell'esperimento 3DOSE

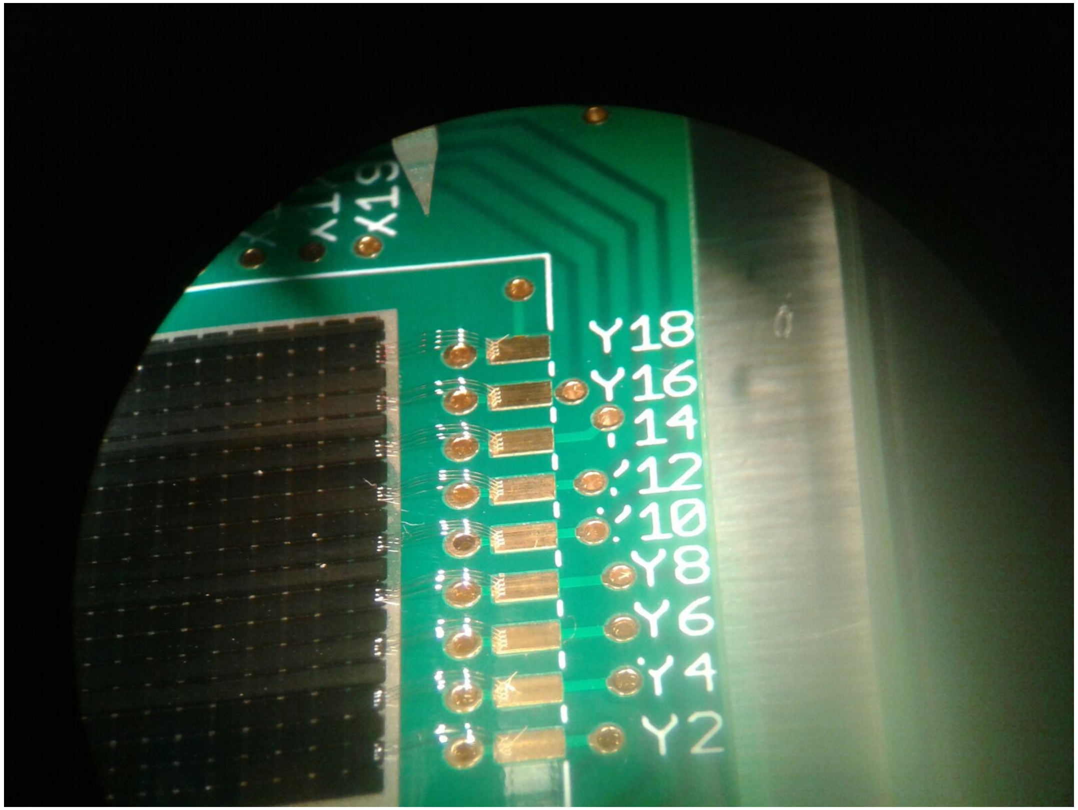

alternativa: scrittura di maschere (incisione su nastro adesivo ultrasottile) e metallizzazione per sputtering su piste grafitiche, con successivo bonding sulla metallizzazione

Alternativa: metal-diamond bonding (richiede ulteriore manpower)

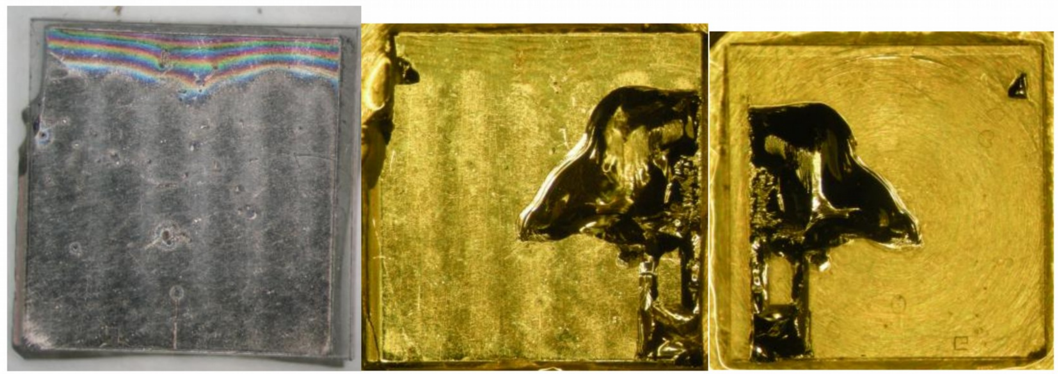

Diamante su Al Alluminio staccato diamante staccato

Bonding silicio-diamante

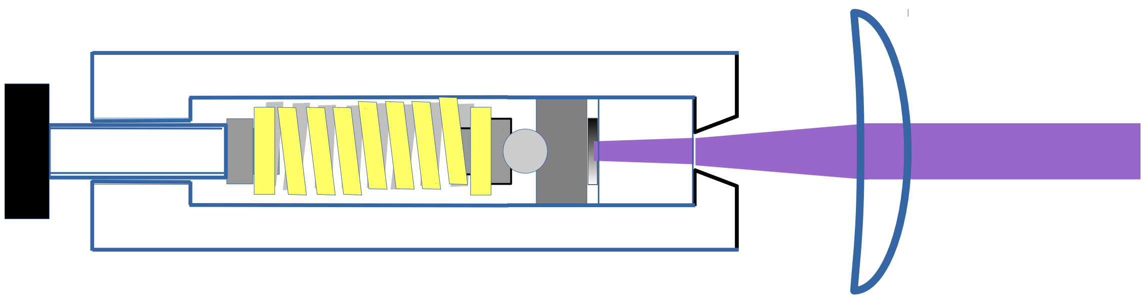

Parametri che si sono usati dal 2013
800 atm, 355 nm, 20 ps, 0.4 J/cm^2

Si possono variare tutti i parametri

Il cambiamento dei parametri è legato al miglioramento delle condizioni di saldatura (*ad esempio: superfici perfettamente lisce implicano pressione zero*)

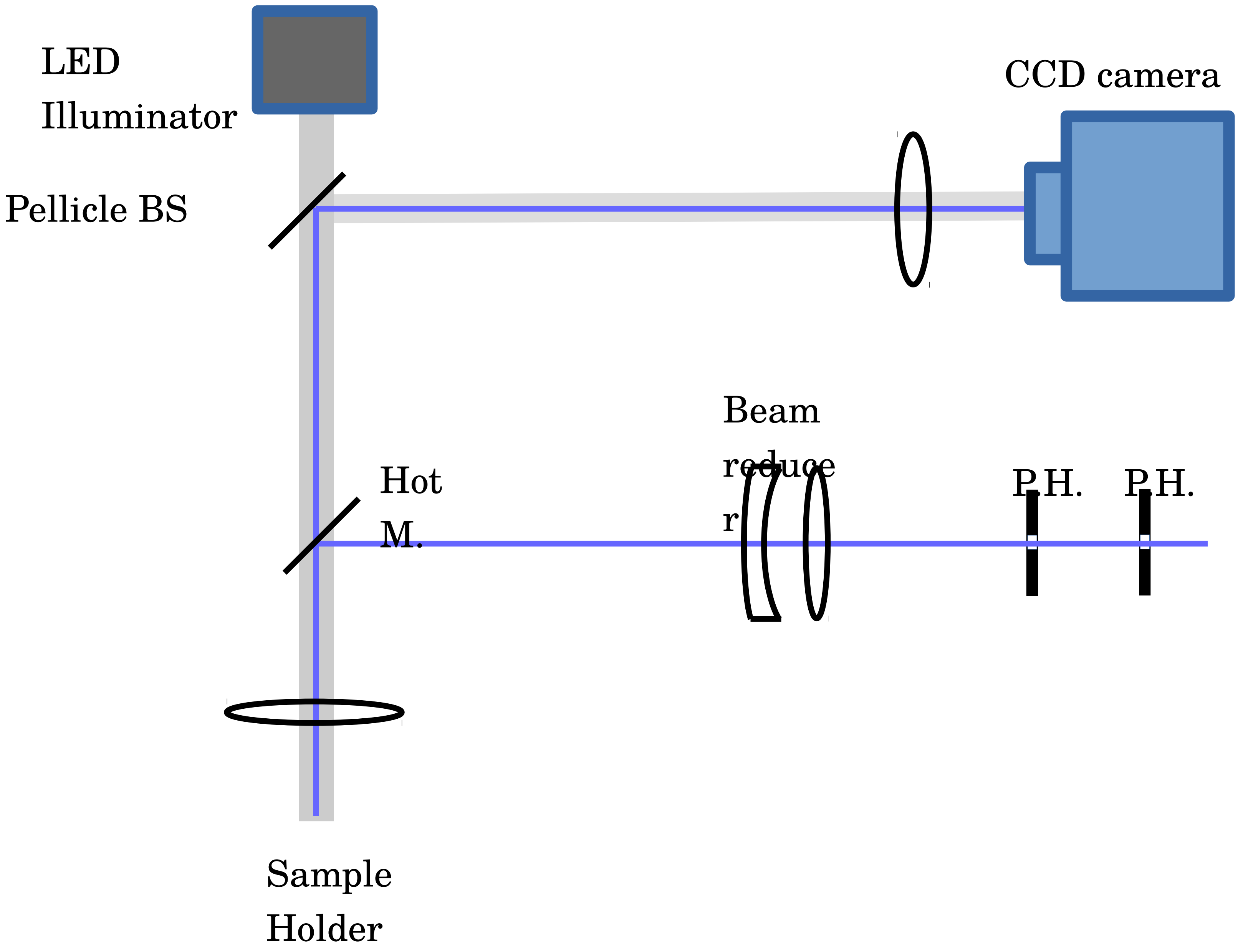

Sistema di saldatura laser silicio-diamnte / metallo-diamante

Irradiation plan extended to monocrystalline and DOI , up to 1.2 n/cm^2 (1 MeV equivalent)

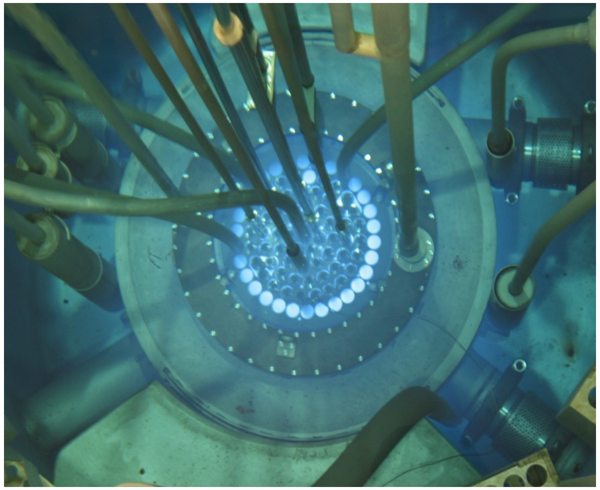

TRIGA reactor JSI Ljubljana (Aida 2020 Transnational access)

Φ fluence ($n\,\mathrm{cm}^{-2}$ 1 MeV)

Polycrystalline	Monocrystalline	DOI
2.6×10^{14}		
	1.25×10^{15}	
3×10^{15}	2.5×10^{15}	2.5×10^{15}
6×10^{15}	5×10^{15}	5×10^{15}
1.2×10^{16}	1×10^{16}	1×10^{16}

$$\frac{1}{\lambda} = \frac{1}{\lambda_0} + k\Phi$$

λ mean free path of electron/holes

k hardness factor

$\frac{1}{\lambda_0} \approx 0$ for monocrystalline

$k = 0.65 - 0.7 \times 10^{-18} \mu m^{-1}\ cm^2$ for 24 GeV protons H Kagan, Diamond Detectors, INFN Summer School, Florence, Italy, June 5, 2012

$k = 5 - 8 \times 10^{-18} \mu m^{-1}\ cm^2$ for 1 MeV neutrons our measurements **7-12 times more effective**

Results of irradiations

Monocrystalline sample, 3D , 500 col/mm^2

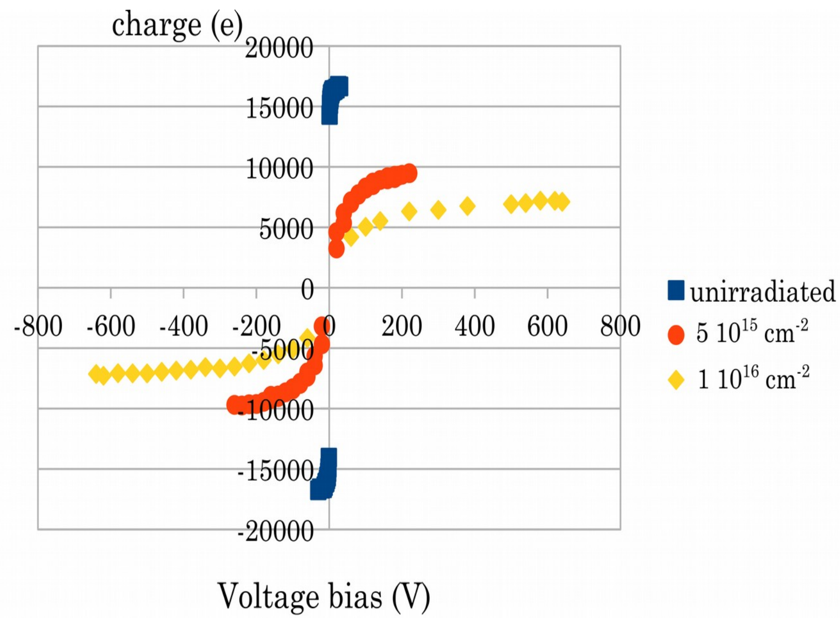

log scale for voltage bias

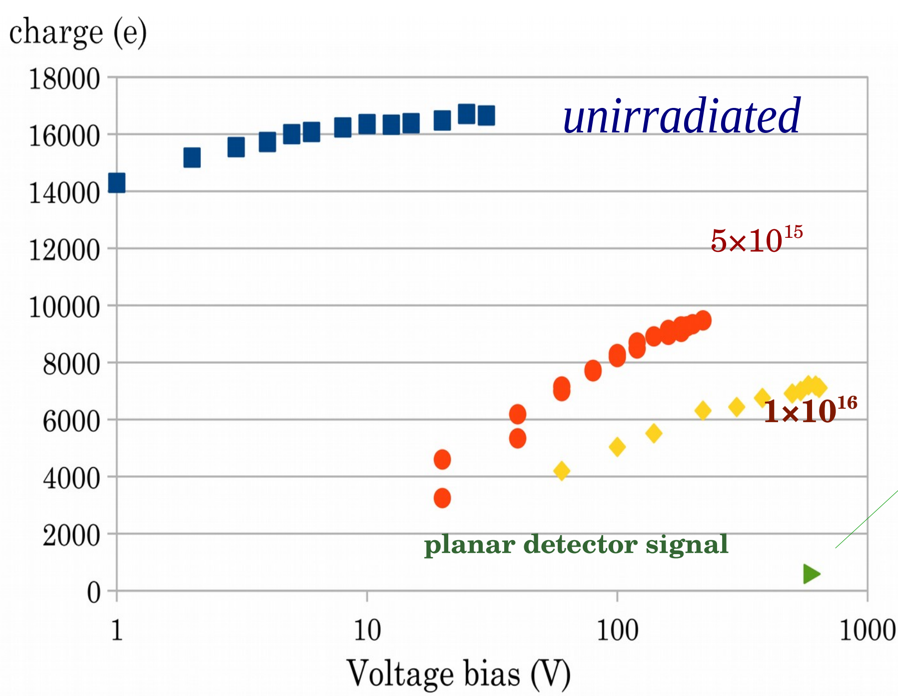

At increasing fluence of irradiation **the maximum applicable voltage increases**

By increasing the applied voltage, **at the highest fluence of 1 10^{16} n/cm^{-2} , it is possible to obtain >40% of the original signal**

After this fluence damage the 2D sensors yields a signal below 600 e

expected noise of ~150 e (depending on pixel capacitance and leakage current)

Leakage currents

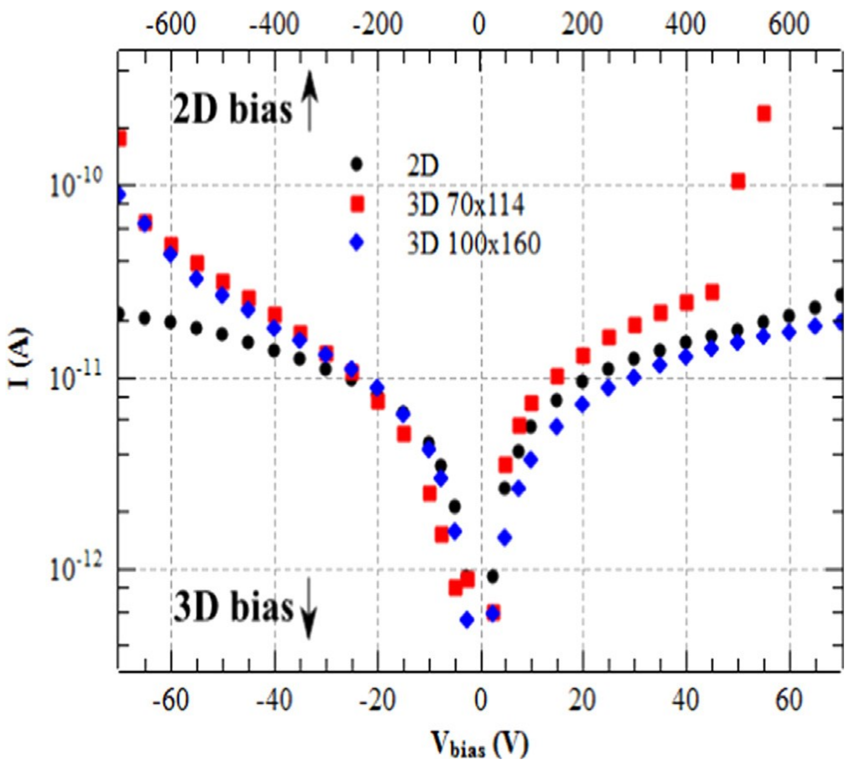

Defect-induced currents currents tend to appear at high voltages, more pronounced with shorter inter-electrode distances

For this reason **it was not possible to apply voltages higher than 70 V to unirradiated 3D detectors**

After the highest irradiations **currents lower than 1 nA (for ~500 electrodes in parallel) @ 650 V bias**

Mechanism of reduction of defect concentration by neutron irradiation have been reported in the past

L. Allers, et al. Diamond Relat. Mater. 6, 353 (1997).

Bruzzi, et al. Applied Phys. Lett. 81.2 (2002): 298-300.

Raw data @70V

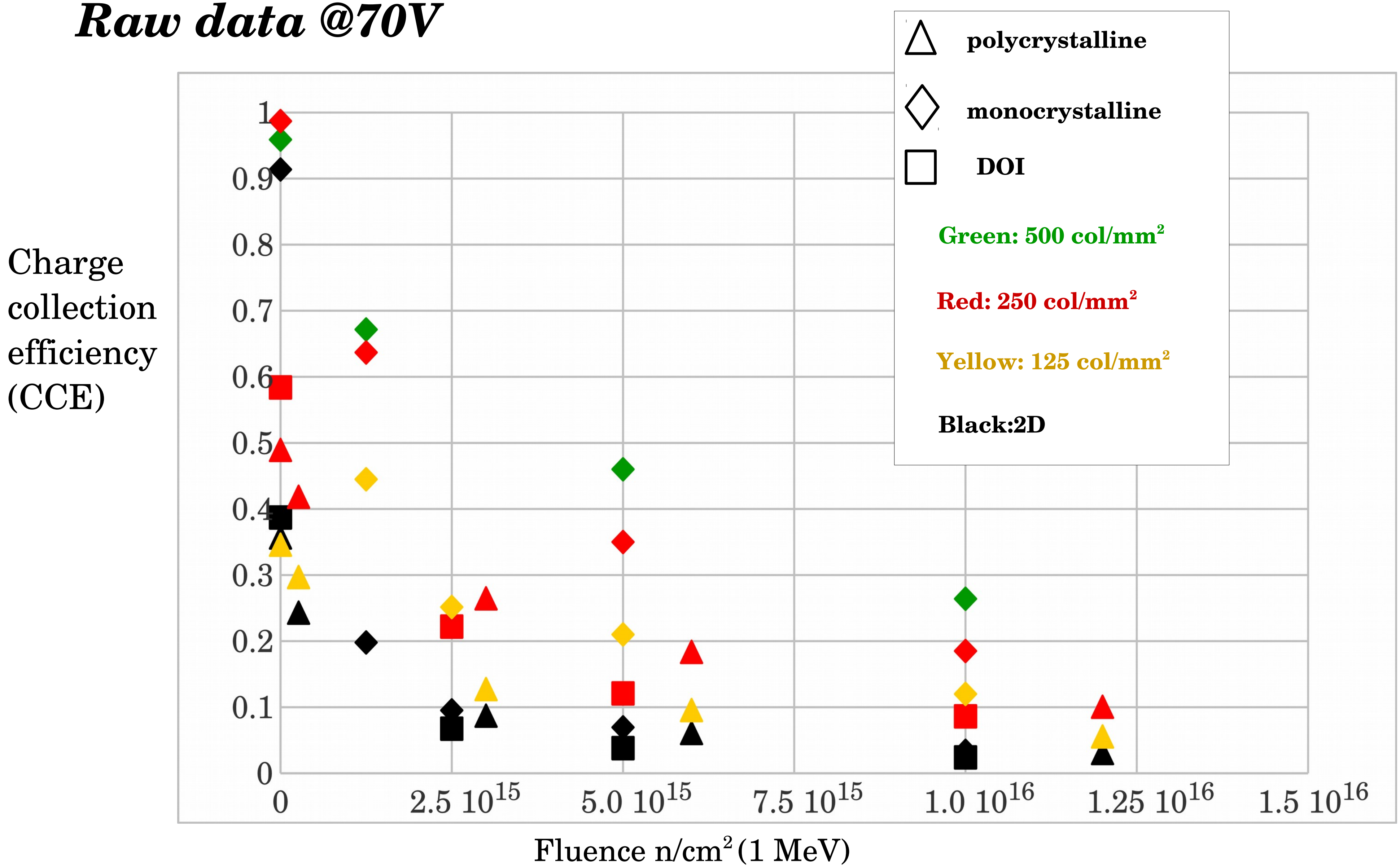

$$\frac{1}{\tau}=\frac{1}{\tau_0}+K\,\Phi=K\left(\Phi_0+\Phi\right)$$

Inefficiency of poly and DOI to be taken into account with effective fluence Φ_0

Data Analysis: 3D detectors

We simulated the charge-collection of 3D-sensors by means of a Monte Carlo algorithm using a three-dimensional finite element calculation of the electric field.

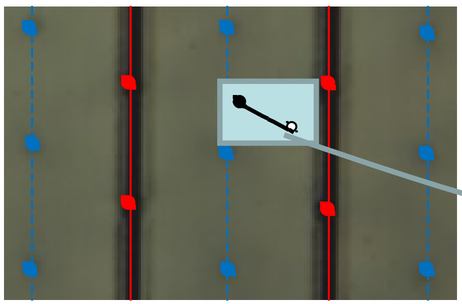

Elem. cell

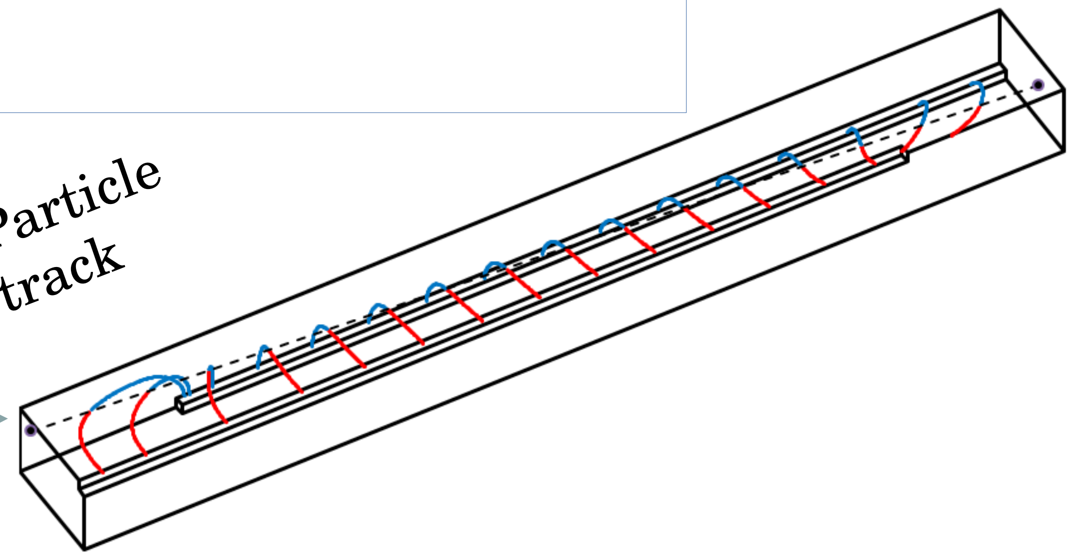

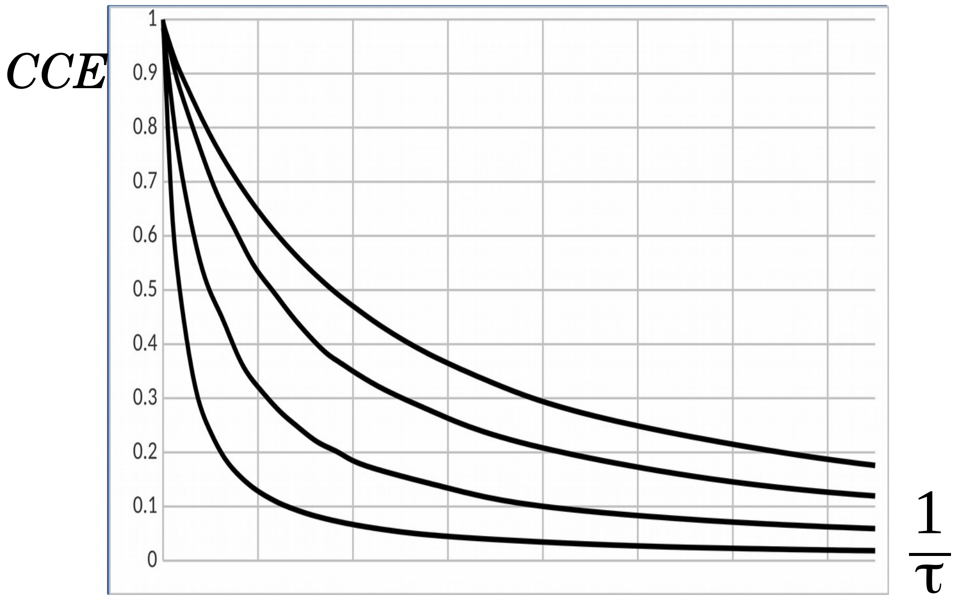

$CCE = f\left(\frac{1}{\tau}\right)$ dependent on 3D pattern and bias

τ is function of Φ: $\frac{1}{\tau} = \frac{1}{\tau_0} + K\Phi$

$CCE = f\left(\frac{1}{\tau_0} + K\Phi\right)$ τ_0, K fit parameters

Raw data @70V

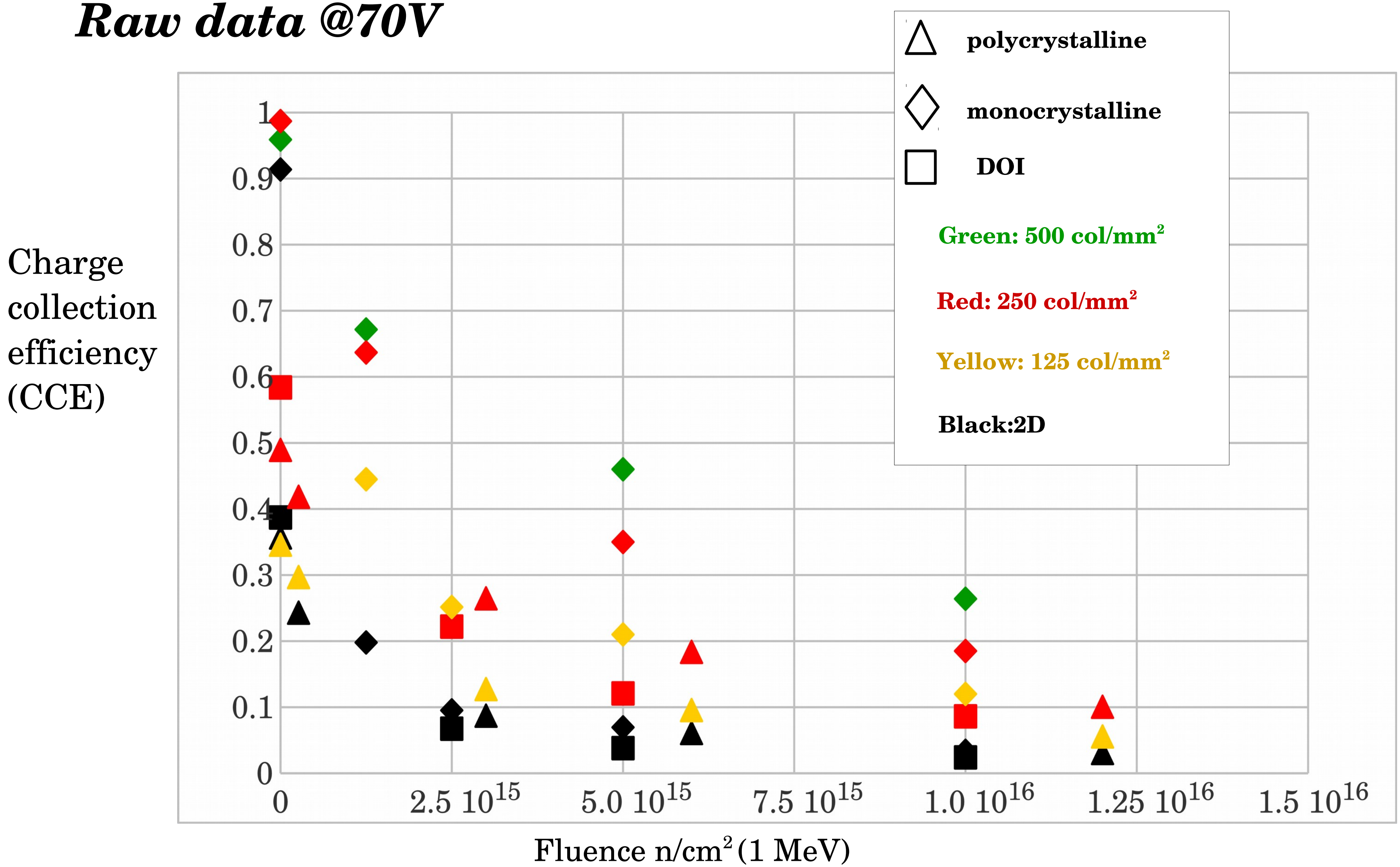

$$\frac{1}{\tau}=\frac{1}{\tau_0}+K\,\Phi=K\left(\Phi_0+\Phi\right)$$

Inefficiency of poly and DOI to be taken into account with effective fluence Φ_0

Data and simulations @ 70 V bias (without 3D DOI)

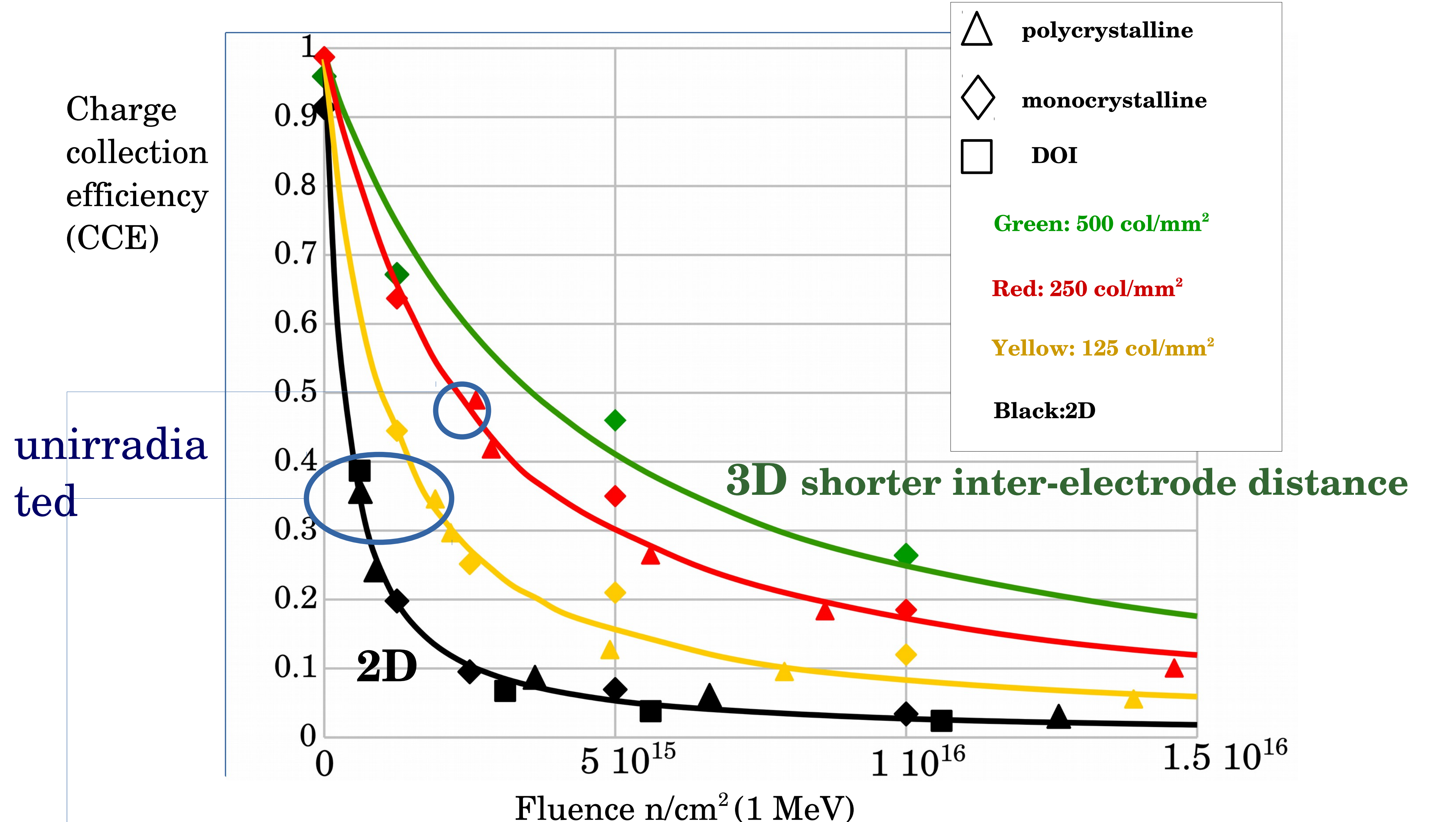

$$\frac{1}{\tau} = K(\Phi_0 + \Phi)$$

Inefficiencies of poly and DOI have been taken into account translating all points by effective fluence Φ_0

Data and simulations @ 70 V bias (without 3D DOI)

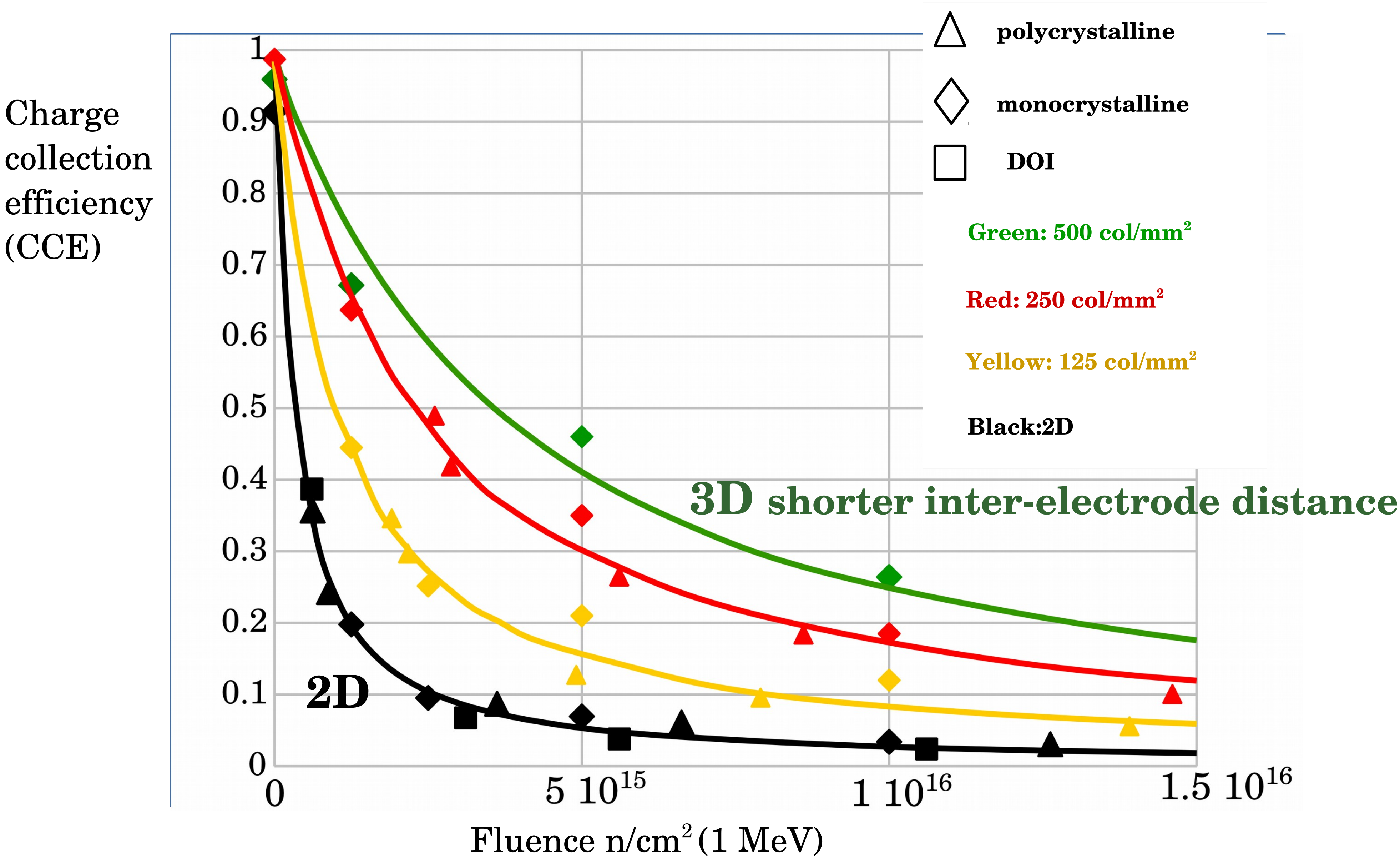

damage constant of poly and mono $K = (1.3 \pm 0.2) \times 10^{-6}\ cm^2 s^{-1}$

Data and simulations for the highest density of electrodes (smaller pitch) @ different bias voltages

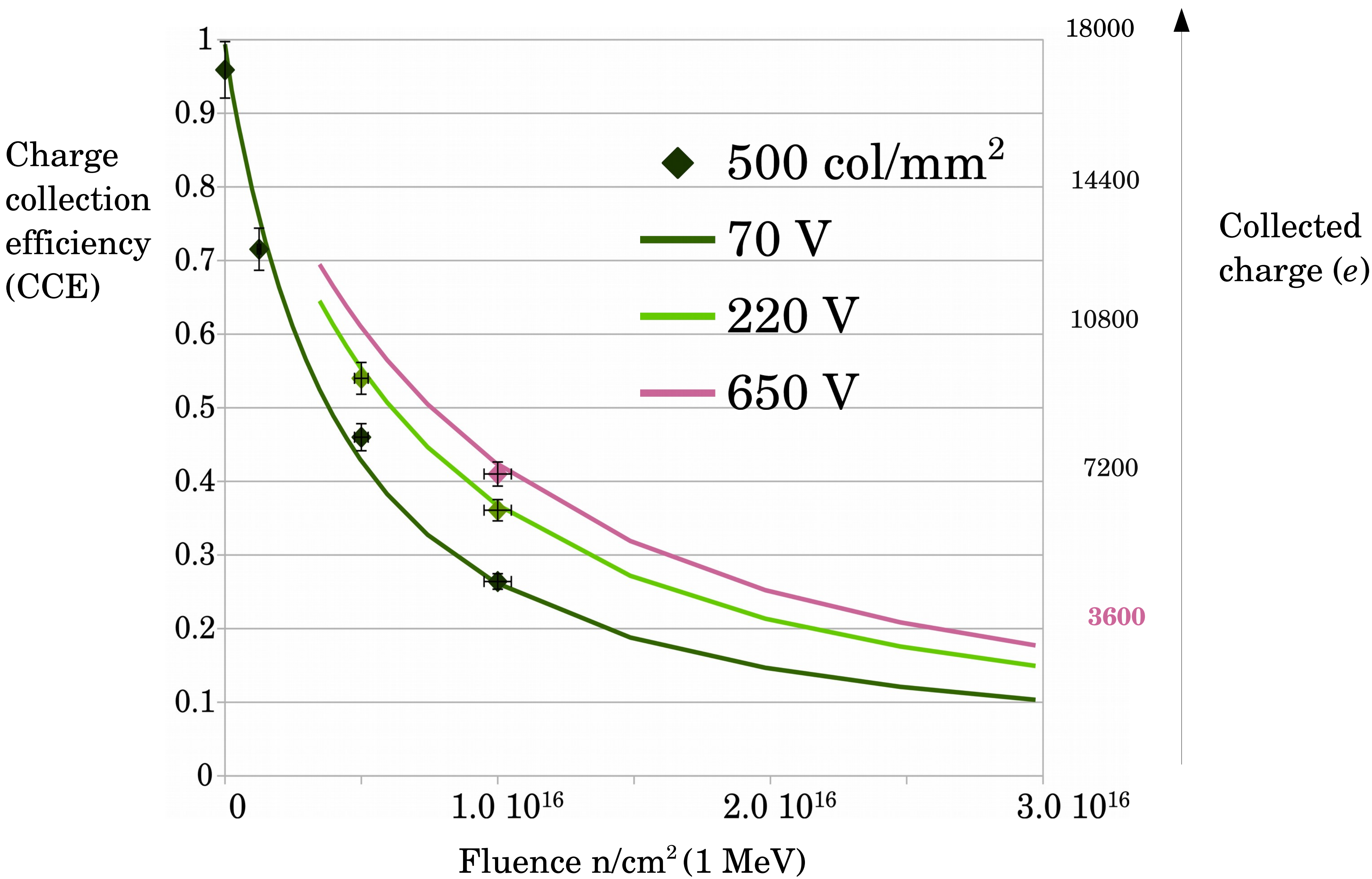

By increasing the voltage bias, the sensor is operative at higher fluences

Data and simulations (3D DOI)

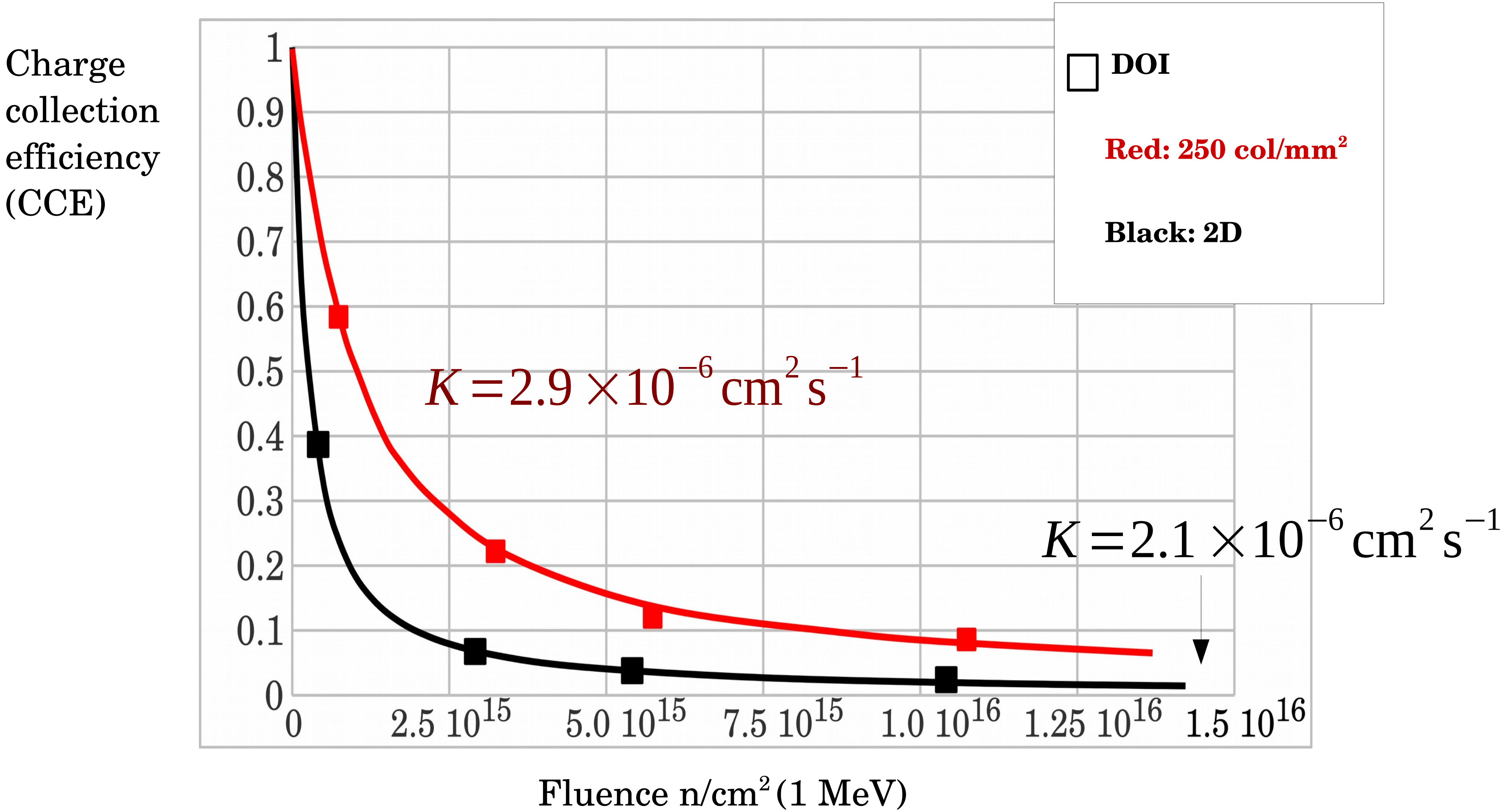

$$\frac{1}{\tau} = K\left(\Phi_0 + \Phi\right)$$

Higher radiation damage for the 3D structure
(to be verified with new generation samples)

Misure preliminari di timing, utillizzando il laser a fs

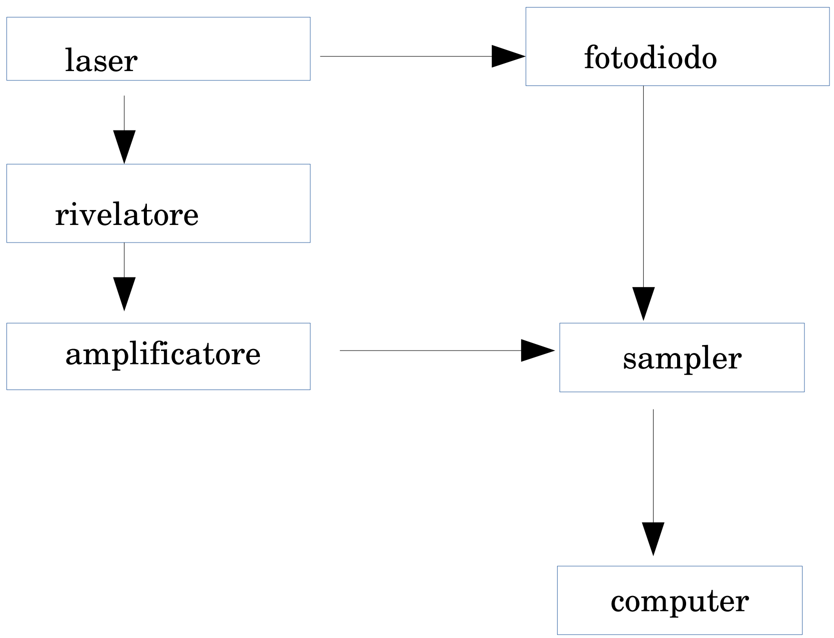

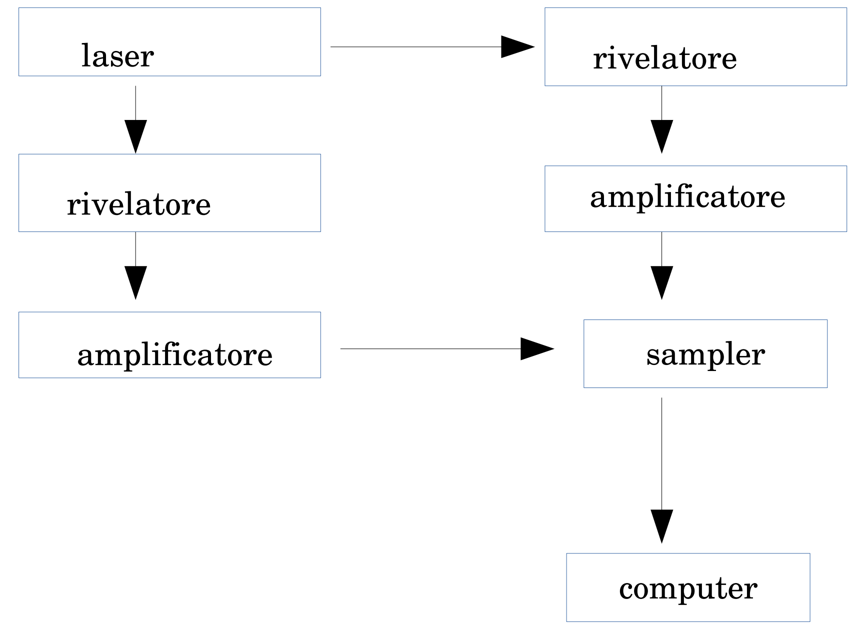

Abbiamo un fotodiodo Thorlabs
InGaAs Pin
750 - 1650 nm

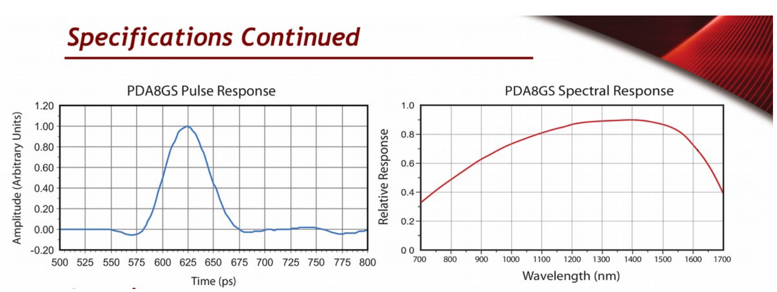

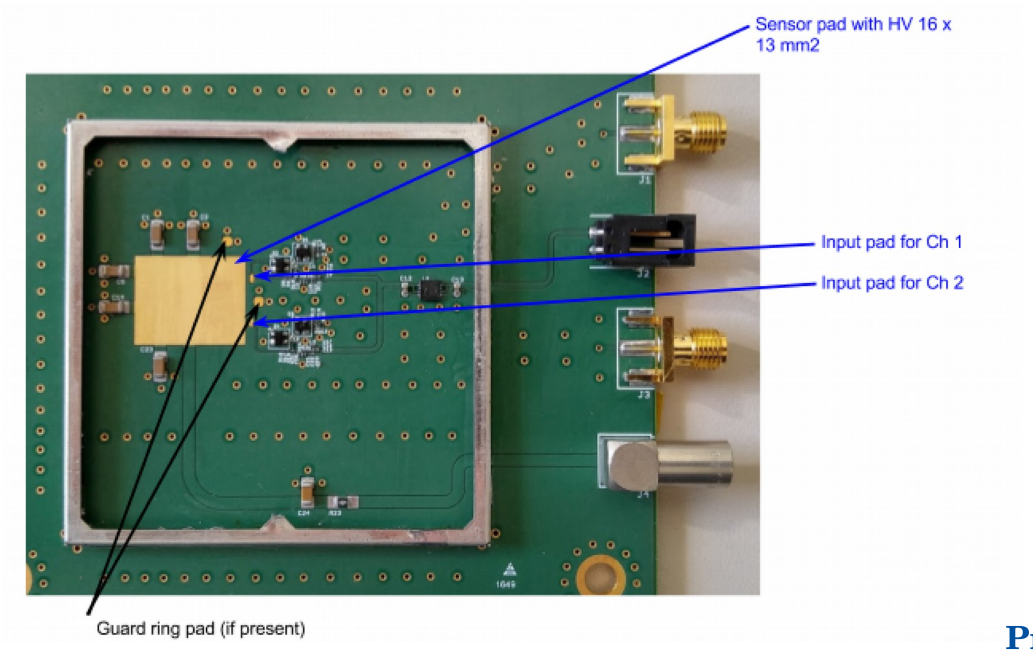

stadio amplificazione Kansas Univ tramite Nicola Minafra TOTEM (Kansas University)

N. Minafra, Test of Ultra Fast Silicon Detectors for Picosecond
Time Measurements with a New Multipurpose Read-Out Board
https://arxiv.org/abs/1704.05298

Precision Electron Polarimetry at EIC, Nicola Minafra, KU

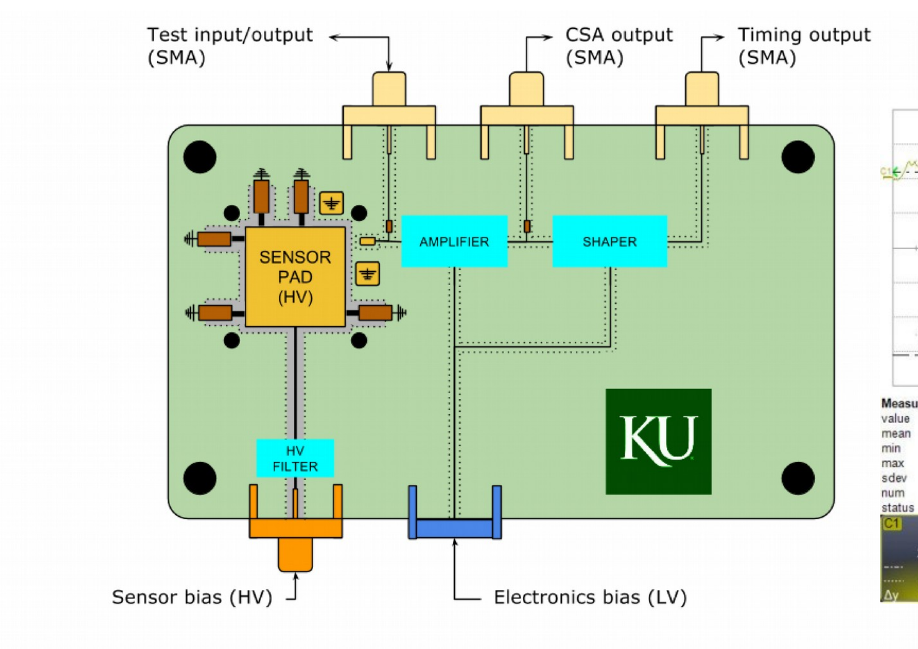

Signal from a 500 um pCVD diamond

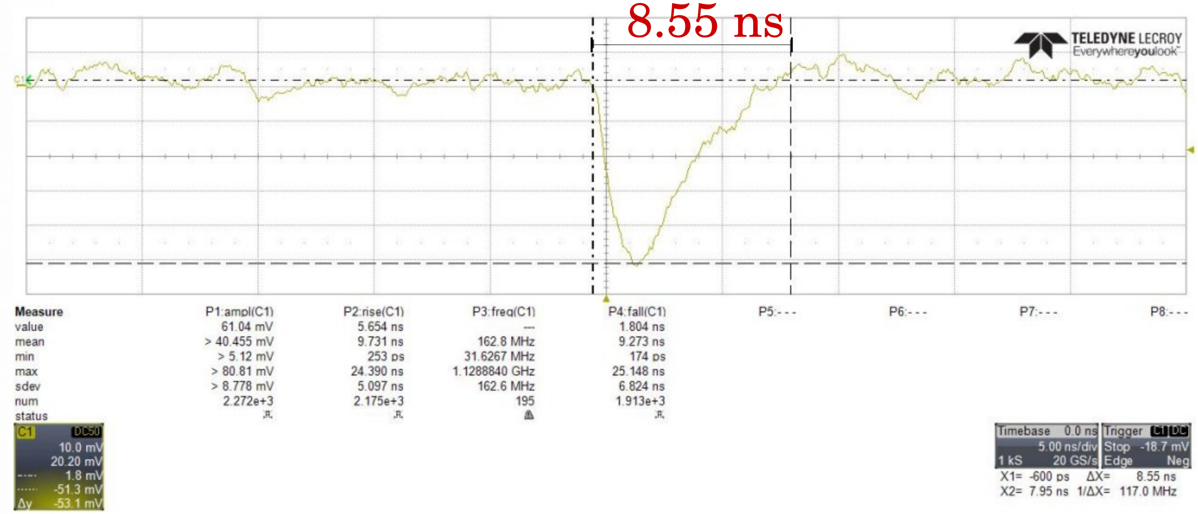

Measure	P1:ampl(C1)	P2:rise(C1)	P3:freq(C1)	P4:fall(C1)	P5:---	P6:---	P7:---	P8:---
value	61.04 mV	5.654 ns	---	1.804 ns				
mean	> 40.455 mV	9.731 ns	162.8 MHz	9.273 ns				
min	> 5.12 mV	253 ps	31.6267 MHz	174 ps				
max	> 80.81 mV	24.390 ns	1.1288840 GHz	25.148 ns				
sdev	> 8.778 mV	5.097 ns	162.6 MHz	6.824 ns				
num	2.272e+3	2.175e+3	195	1.913e+3				
status								

costo realizzazione

Link Engineering srl
Via Parini, 1 - 40033
Casalecchio di Reno (BO)
Tel. +39 051 6414051

Uffici Milano:
Via IV Novembre, 92
Edificio C
20021 Bollate (MI)

Uffici Genova:
Via Fiumara 3/2
Torre mare
16149 Genova

Cliente	Offerta	Oggetto
CERN - SITE DE MEYRIN CH-1211 Geneve 23 Switzerland	N° JC16-507 28/11/2016 Validità 30 gg	Board Kuamplifier_v2 Production 6pz / 10pz / 20pz Att.ne Mr. Nicola Minafra

Pos.	Q.tà	Descrizione	Prezzo Unitario	Prezzo Totale	Consegna
1	1	Production 6pz Supply PCB. Supply of all components listed in the BOM parts in our possession. Setup P / P. Complete assembly and Analysis AOI / X-Ray Visual inspection and packing mat. antistatic.		€1.950,00	T0 + 4 wks
2	1	Production 10pz Supply PCB. Supply of all components listed in the BOM parts in our possession. Setup P / P. Complete assembly and Analysis AOI / X-Ray Visual inspection and packing mat. antistatic.		€2.280,00	T0 + 4 wks
3	1	Production 20pz Supply PCB. Supply of all components listed in the BOM parts in our possession. Setup P / P. Complete assembly and Analysis AOI / X-Ray Visual inspection and packing mat. antistatic.		€2.720,00	T0 + 4 wks

Delivery to CERN (IVA free)

Condizioni Generali di Fornitura

Consegne: As reported in the individual positions
Pagamenti: B.B. 30 gg F.M.
Resa: Transport and packaging included
Garanzia Prototipi o Produzione: 12 months
Garanzia Ingegneria Industriale: The provision is in compliance with applicable laws in terms of safety.

Link Engineering S.r.l.
Roberto Baldazzi

Waveform digitizer SAMPIC (circa 3000 euro)

Measurements of timing resolution of ultra-fast silicon detectors with the SAMPIC waveform digitizer
arXiv:1604.02385

a series of delay lines control a network of capacitors (64 per channel) that continuously samples the input signal with a frequency up to 10 GSa/s

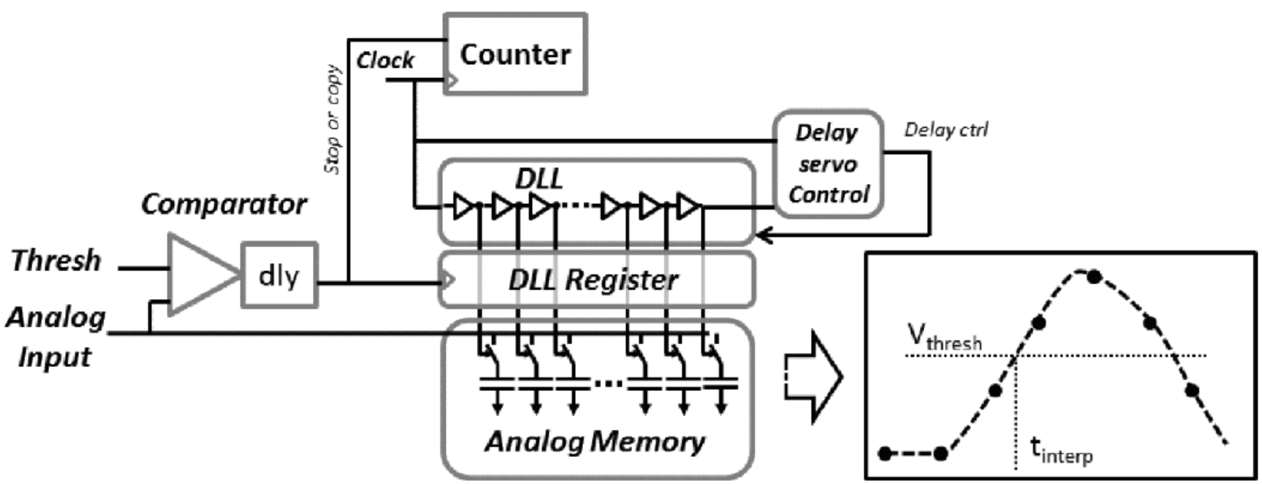

Spare slides

Charge Collection Efficiency (CCE) Measurement

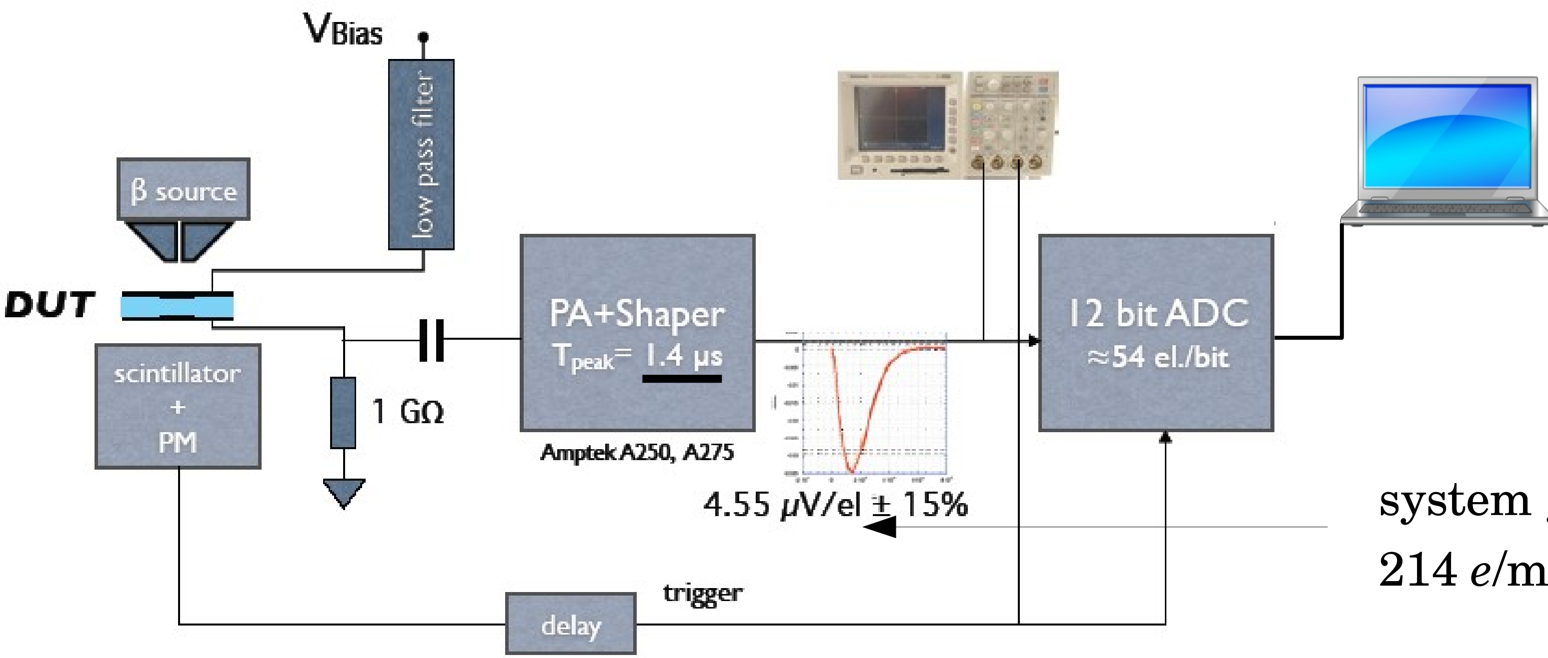

system gain:

214 e/mV

Average generated charge
in a monocrystalline test sample
$500\,\mu\text{m} \times 36\, e-h$ pairs $/\,\mu\text{m} = 18000$ e

pairs created by a Minimum Ionizing Particle (MIP)

Bias is periodically inverted to prevent polarization effects, present at low bias voltage

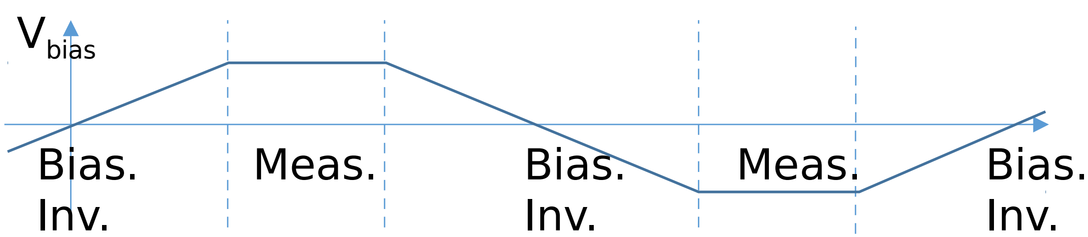

PDA8GS

The PDA8GS is a versatile, high-speed, amplified photodetector designed to perform in a wide range of test and measurement applications involving fast optical signals. The unit incorporates a high-performance InGaAs PIN photodiode coupled with a transimpedance amplifier that has a gain of 460 V/A into 50 Ω with data rates up to 12.5 Gb/s. The wide bandwidth makes it ideal for evaluating pulsed laser and high-frequency modulation applications. Communication applications include 10 Gb Ethernet, OC192, and analog satellite microwave systems. This model exhibits linear performance across the input range, yielding low analog distortion. A 12 VDC, 750 mA power adapter is included with the PDA8GS. The housing features an FC bulkhead connector, which is compatible with both FC/PC and FC/APC connectors.

We can control the pulse compression (i.e. Pulse duration) by varying the position of a couple of prisms (P1-P2), and we can measure the pulse lenght τ by means of a Michelson correlator.

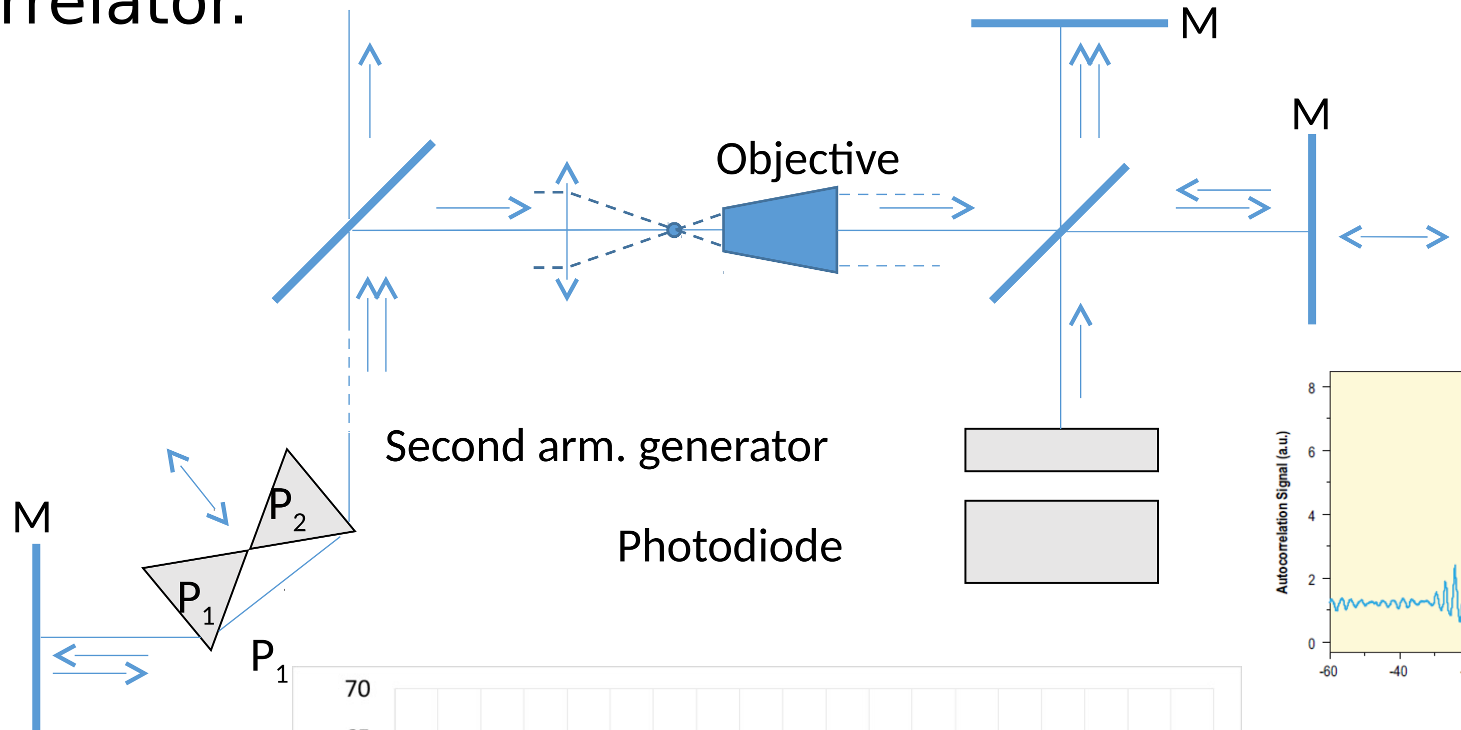

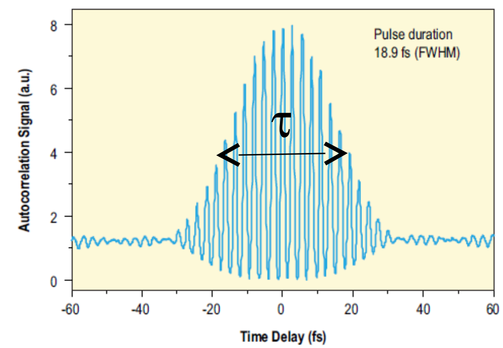

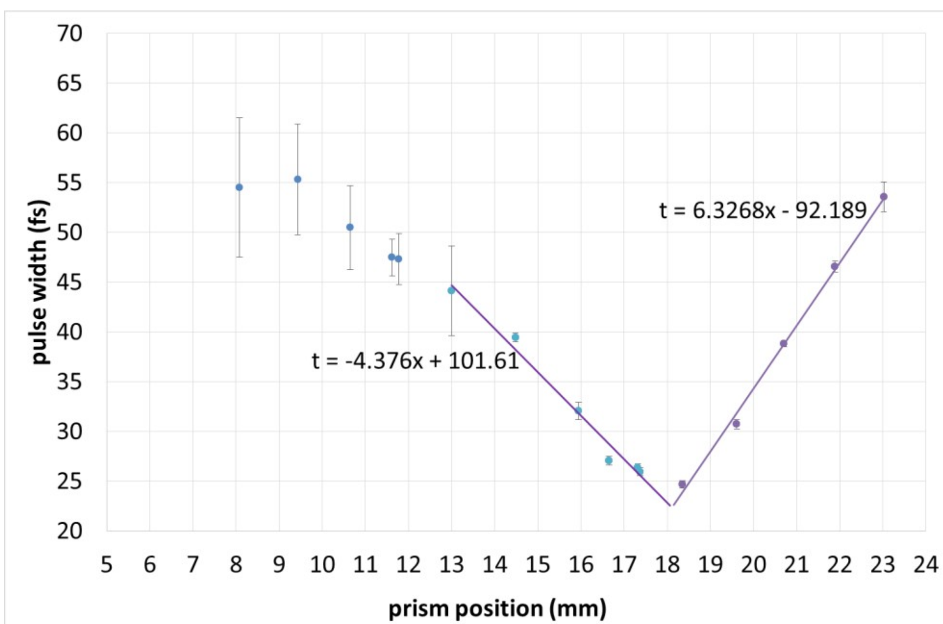

In this way we can fabricate columns with given E and τ

The setup of an interferometric autocorrelator (Figure) contains a Michelson interferometer with a variable arm length difference. The superimposed copies of the pulse are collinearly propagating into the nonlinear crystal (after focusing with a lens or curved laser mirror) and have the same polarization.

An interferometric autocorrelation is obtained by recording the average power of the frequency-doubled signal:

$$\int (E(t)+E(t+\tau))^4 \, dt$$

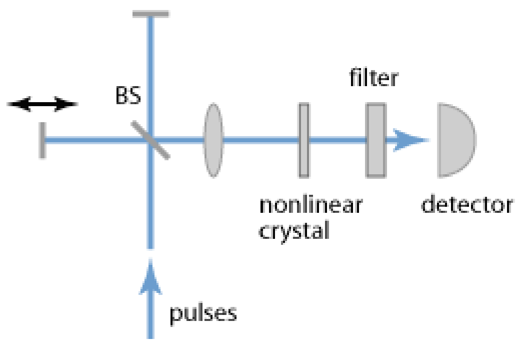

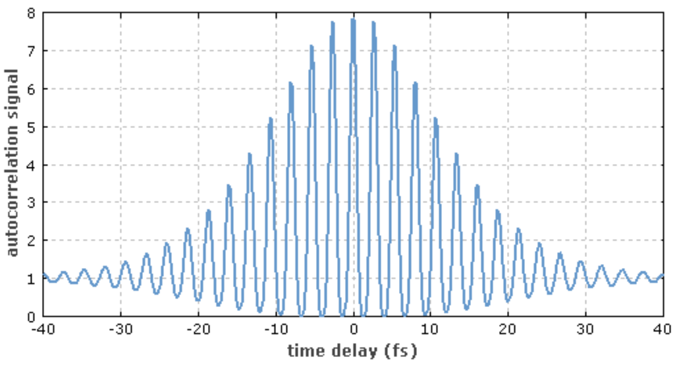

This kind of autocorrelation trace exhibits a fast oscillation with a period of half the optical wavelength. The maximum signal is obtained when the two pulses after the beam splitter undergo perfect constructive interference, leading to twice the amplitude compared with a single pulse, and thus four times the intensity, and after frequency doubling 16 times the intensity. For a large arm length difference, the pulses do not overlap in the nonlinear crystal, and the intensity is only twice that generated by a single pulse. Hence the peak signal is always eight times higher than the background, provided that the interferometer is properly aligned.

We also take into account the pattern of the RAPS electronics

Using a gold buffer to make the pressure more uniform

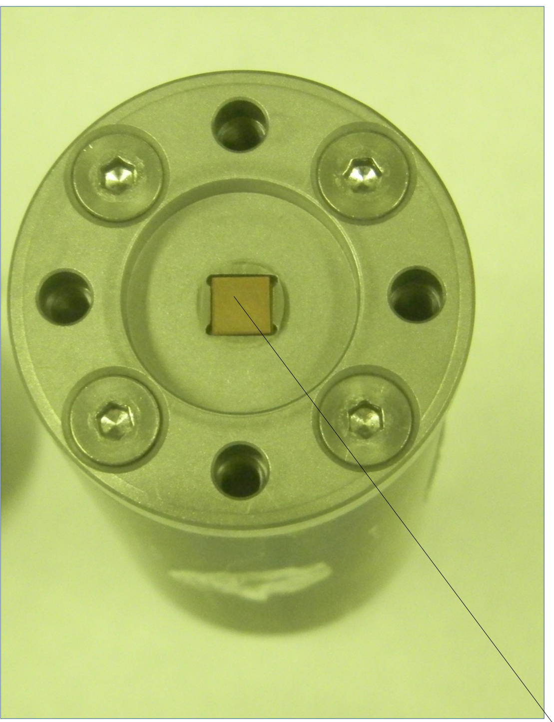

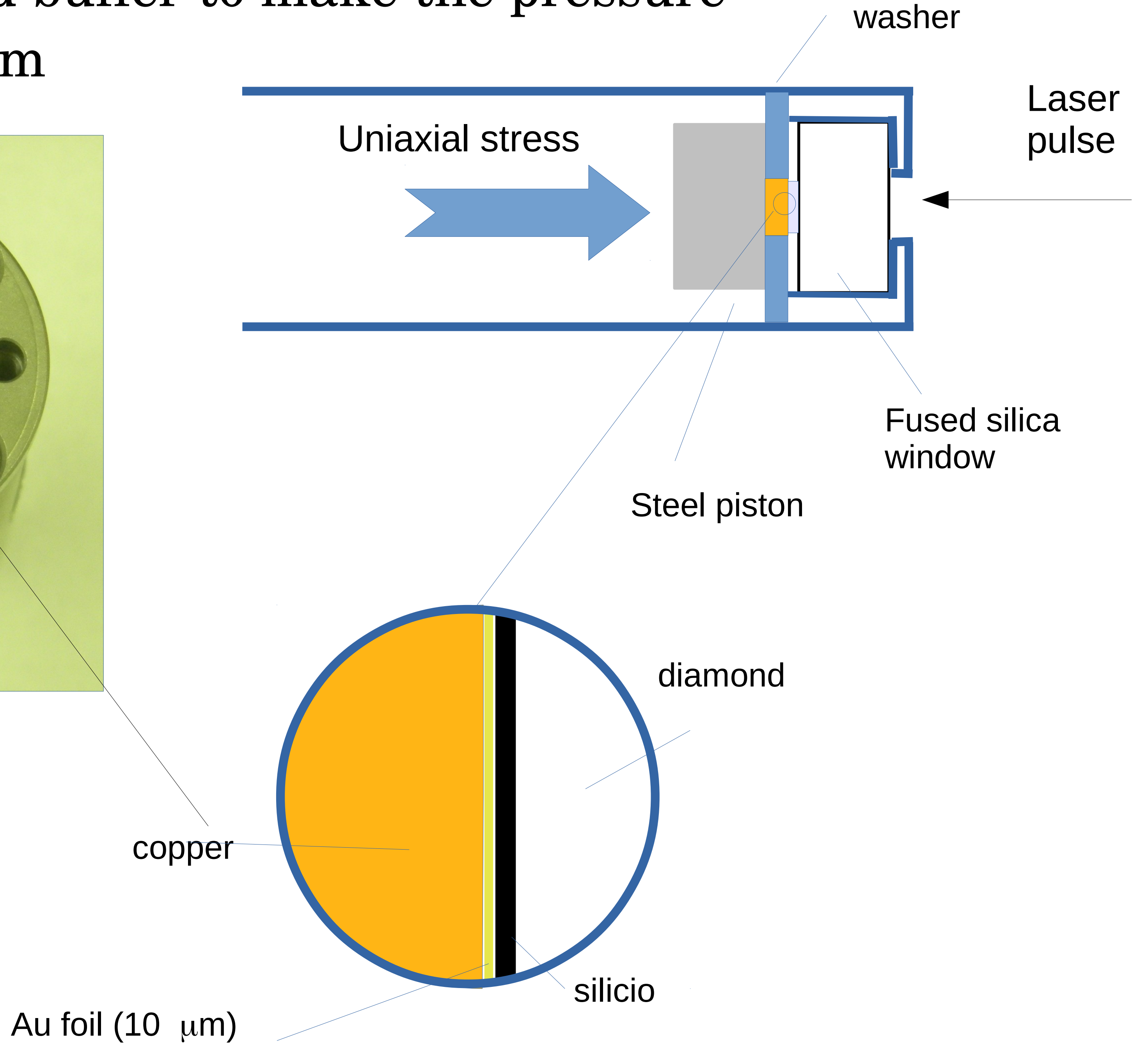

dispositivo integrato silicio-diamnte

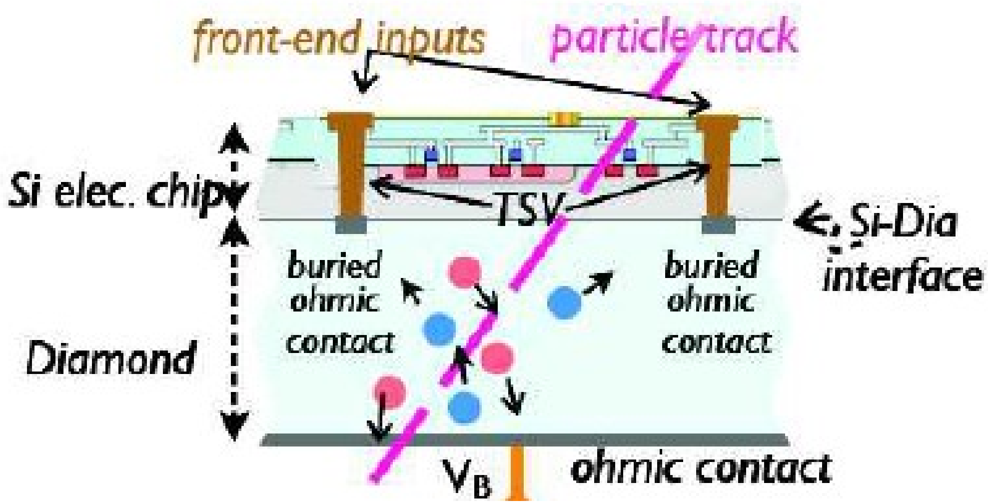

Chip-On-Diamond
Da esperimento CHIPSODIA
(2010-2013)